

Megafauna of vulnerable marine ecosystems in French mediterranean submarine canyons: Spatial distribution and anthropogenic impacts

M-C. Fabri^{a,*}, L. Pedel^a, L. Beuck^b, F. Galgani^a, D. Hebbeln^c, A. Freiwald^{b,c}

^a Ifremer, Département Océanographie et Dynamique des Ecosystèmes, 83500 La Seyne sur Mer, France

^b Senckenberg am Meer, Marine Research Department, Südstrand 40, 26382 Wilhelmshaven, Germany

^c MARUM – Center for Marine Environmental Sciences, Leobener Strasse, 28359 Bremen, Germany

*: Corresponding author : Marie-Claire Fabri, tel.: +33 4 94 30 48 05; fax: +33 4 94 30 44 17 ;
email address : Marie.Claire.Fabri@ifremer.fr

Abstract:

Vulnerable Marine Ecosystems (VME) in the deep Mediterranean Sea have been identified by the General Fisheries Commission for the Mediterranean as consisting of communities of Scleractinia (*Lophelia pertusa* and *Madrepora oculata*), Pennatulacea (*Funiculina quadrangularis*) and Alcyonacea (*Isidella elongata*). This paper deals with video data recorded in the heads of French Mediterranean canyons. Quantitative observations were extracted from 101 video films recorded during the MEDSEACAN cruise in 2009 (Aamp/Comex). Qualitative information was extracted from four other cruises (two Marum/Comex cruises in 2009 and 2011 and two Ifremer cruises in 1995 and 2010) to support the previous observations in the Cassidaigne and Lacaze-Duthiers canyons. All the species, fishing impacts and litter recognized in the video films recorded from 180 to 700 m depth were mapped using GIS. The abundances and distributions of benthic fishing resources (marketable fishes, Aristeidae, Octopodidae), Vulnerable Marine Species, trawling scars and litter of 17 canyons were calculated and compared, as was the open slope between the Stoechades and Toulon canyons. *Funiculina quadrangularis* was rarely observed, being confined for the most part to the Marti canyon and, *I. elongata* was abundant in three canyons (Bourcart, Marti, Petit-Rhône). These two cnidarians were encountered in relatively low abundances, and it may be that they have been swept away by repeated trawling. The Lacaze-Duthiers and Cassidaigne canyons comprised the highest densities and largest colony sizes of scleractinian cold-water corals, whose distribution was mapped in detail. These colonies were often seen to be entangled in fishing lines. The alcyonacean *Callogorgia verticillata* was observed to be highly abundant in the Bourcart canyon and less abundant in several other canyons. This alcyonacean was also severely affected by bottom fishing gears and is proposed as a Vulnerable Marine Species. Our studies on anthropogenic impacts show that seafloor disturbance by benthic fishing is mainly attributable to trawling in the Gulf of Lion and to long lines where rocky substrates are present. The bauxite residue (red mud) expelled in the Cassidaigne canyon was seen to prevent fauna from settling at the bottom of the canyon and it covered much of the flanks. Litter was present in all of the canyons and especially in considerable quantities in the Ligurian Sea, where the heads of the canyons are closer to the coast. Three Marine Protected Areas and one fishing area with restricted access have recently been established and should permit the preservation of these deep ecosystems.

Keywords : Seafloor mapping ; Biodiversity ; Bathyal-benthic zone ; Cold-water coral ; Litter ; Fishing impact ; Bauxite red mud waste ; Mediterranean Sea ; French submarine canyons (43°N, 5°E)

56
57
58
59
60
61
62
63
64
65
66
67
68
69
70
71
72
73
74
75
76
77
78
79
80
81
82
83
84
85
86
87
88
89
90
91
92
93
94
95
96
97
98
99
100
101
102
103
104
105
106
107
108
109
110

1. Introduction

There has been increasing societal demand for the conservation of biodiversity since the Convention on Biological Diversity recognised the intrinsic value of biological diversity and its ecological, genetic, social, economic, scientific, educational, cultural and recreational benefits at the 1992 Earth Summit in Rio de Janeiro (<http://www.cbd.int/>). Considerable efforts have been made in recent years through the ten-year Census of Marine Life Project to estimate biodiversity in the oceans (Costello et al., 2010). Nevertheless the total number of marine species is still unknown because many species remain to be sampled, distinguished and described (Bouchet, 2006). Less is known about deep-sea areas compared to coastal environments due to the practical difficulties of sampling deeper waters. However, there is a pronounced shift of fisheries from shallow to much deeper regions, motivated by the declining fish stocks on the continental shelves (Cartes et al., 2004) and by the advanced fishing gear technology now available for the efficient exploitation of the bathyal zone. Despite this, deep-water ecosystems are characterized by low productivity, low fecundity, older age at first maturity and high longevity of the species adapted to these environments; thus they are highly sensitive to commercial exploitation.

Adverse impacts to Vulnerable Marine Ecosystems (VME) in the deep sea have now become an international concern since the United Nations called on governments and Regional Fishery Management Organisations to prevent them (United Nation, 2007). The Food and Agriculture Organisation (FAO) has formulated management guidelines, by setting up an international consultative process and determining criteria for defining VMEs (FAO, 2009). The latter include uniqueness or rarity of species or habitat, their functional significance, fragility and structural complexity, and life histories that limit the probability of recovery. Examples of taxa indicative of a VME are given associated with specific undersea landscape types, but no explicit metrics, threshold values, or analytical approaches are given for identifying whether one area contains a VME and another does not (Auster et al., 2011). The biggest constraints in protecting VMEs are the uncertainties in the distribution and abundance of VME indicator species, and similar uncertainties in the link between fishing intensity and significant adverse impacts. The Convention for the Protection of the Marine Environment of the North-East Atlantic (OSPAR for Oslo-Paris) has worked to identify the threats to the marine environment and has pioneered the development of methods for monitoring and assessing the quality status of seas. The OSPAR Commission has established a list of threatened and/or declining species and habitats in the OSPAR maritime area that require protection. The deep-sea habitats mentioned in the OSPAR list are coral gardens, *Lophelia pertusa* reefs, deep-sea sponge aggregation and sea-pen and burrowing megafauna communities (<http://www.ospar.org>).

Compared to the adjacent deep Atlantic basins the Mediterranean Sea is a warm, deep, oligotrophic basin where temperatures remain largely uniform but at much higher levels, i.e. around 12.5-14.5°C below 150 m, with high salinity (38.4-39.0) and high oxygen levels (4.5-5.0 ml. l⁻¹) (Cartes et al., 2004). The western Mediterranean basin is connected to the Atlantic by the narrow Strait of Gibraltar, with a sill depth of about 300 m, and to the eastern Mediterranean basin by the Sicily Channel (400 m). These gateways funnel the entire exchange of water mass between the eastern and western basin (Sicily Channel) and with the Atlantic Ocean (Strait of Gibraltar), thereby following the pattern of anti-estuarine circulation (Astraldi et al., 1999). These features distinguish Mediterranean deep-sea communities as being potentially unique and particularly sensitive to human activities. The continental shelves are narrow, except close to the outlets of major rivers (the Rhône in the western basin) (Cartes et al., 2004) and are incised by numerous submarine canyons. Much of the Mediterranean coast has deep-water bottoms near the shore, typically reached within a few hours by commercial vessels. The Mediterranean stands out as a globally different region because its canyons are more closely spaced (14.9 km), more dendritic (12.9 limbs per 100,000 km²), shorter (mean length of 26.5 km) and steeper (mean slope of 6.5°) than canyons found in other regions of the world (Harris and Whiteway, 2011).

The General Fisheries Commission for the Mediterranean (GFCM) has issued a list of criteria for the identification of sensitive habitats of relevance for the management of priority species in the Mediterranean Sea (GFCM, 2009a). The GFCM has also issued a list of identified sensitive habitats including: (1) cold-water corals (*Lophelia pertusa* and *Madrepora oculata* communities) which form

111 colonies supported by a common skeleton, providing a structural habitat for other species (Peres and
112 Picard, 1964; Zibrowius, 1980); (2) soft mud facies with *Funiculina quadrangularis* (Bellan-Santini et
113 al., 2002; Peres and Picard, 1964), which is an essential habitat for certain crustacean species
114 (*Parapenaeus longirostris* and *Nephrops norvegicus*); and (3) compact mud facies with *Isidella*
115 *elongata* (Bellan-Santini et al., 2002; Maurin, 1962; Peres and Picard, 1964), which is a relevant
116 habitat for red shrimps (*Aristeus antennatus* and *Aristaeomorpha foliacea*). These habitats are
117 potentially vulnerable as they are targeted by fisheries. Another anthropogenic pressure affecting
118 seafloor integrity includes silting which can change the environmental conditions of the habitats. For
119 instance the Cassidaigne canyon, near Marseille, France, has received red mud discharged by the
120 Gardanne Aluminium factory since 1967. Red mud extends into the abyssal plain more than 50 km
121 away from the pipe (Dauvin, 2010; Fontanier et al., 2012).

122 All the pressures on natural marine resources and the demand for marine ecological services are
123 considered excessive and have led to the establishment of the European Marine Strategy Framework
124 Directive (MSFD). This marine environmental policy established in 2008 aims at reducing impacts on
125 marine waters, by considering that the marine environment is a precious heritage that must be
126 protected, preserved and, where practicable, restored, with the ultimate aim of maintaining
127 biodiversity and providing diverse and dynamic oceans and seas which are clean, healthy and
128 productive. The final objective of the MSFD is to achieve or maintain good environmental status in
129 the marine environment by 2020 at the latest. The work described in this paper was performed in the
130 framework of the initial assessment of the bathyal benthic ecosystems in the French submarine
131 canyons of the Mediterranean Sea.

132 We used a Geographic Information System (GIS) to map all the species and ecosystems
133 recognized on video films recorded during the MEDSEACAN cruise in 2009 (Watremez, 2012), the
134 MARUM cruise in 2009, the MARUM-Senckenberg cruise in 2011, the Ifremer ESSROV cruise in
135 2010 and the CYATOX cruise in 1995. We assessed their spatial distribution from 180 m to 700 m
136 depth in the heads of French canyons. Three objectives were pursued: (1) mapping benthic fishing
137 resources; (2) mapping Vulnerable Marine Ecosystems recognised by the General Fisheries
138 Commission for the Mediterranean (GFCM, 2009a); and (3) assessing the distribution and threat of
139 anthropogenic impacts on benthic ecosystems including fishing activities and waste disposal.

142 2. Materials and methods

144 2.1 Study area

146 The study area covers the shelf break and the bathyal zone of the French continental margin of
147 the northwest Mediterranean Sea, stretching from 42°30'N to 43°30'N and from 3 to 7°E. This
148 continental slope is divided into two regions, namely the Gulf of Lion and the French Riviera
149 (Ligurian Sea). The Gulf of Lion has a broad shelf (wider than 100 km) with a gentle slope, stretching
150 from the coast to the shelf break. The continental shelf off the French Riviera is narrow (2-20 km
151 wide) with a steep slope. The French continental slope is dissected by several canyons in the
152 Mediterranean Sea (from 180 to 2000 m). Seventeen were taken into account in this study, as was the
153 open slope between the Toulon and Stoechades canyons (Fig. 1).

154 Water circulation is generally westward along the continental slope and is constrained by two
155 dominant winds: north-northwesterly winds (upwelling favourable winds) and southeasterly winds
156 (downwelling favourable winds). Prevailing winds from north-west to west (Mistral) cause the
157 displacement of warm surface waters to the open sea, generating six upwelling locations in the Gulf of
158 Lion (Millot, 1990). In combination with the morphology of the coast-line, the Mistral leads to the
159 most intense upwelling of the Gulf of Lion, which rises from the Cassidaigne canyon off Marseille
160 (Alberola and Millot, 2003). During winter, both heat loss and evaporation lead to the cooling and
161 mixing of the coastal waters in the Gulf of Lion. These cold shallow waters finally become denser than
162 the surrounding waters and sink, forming currents known as dense shelf water cascades (DSWC).
163 They carry huge amounts of sediment and organic matter to the deep ocean as they scour the shelf and
164 seafloor slope while sinking. The source area of DSWC is located off Perpignan in the Gulf of Lion
165 (Canals et al., 2006; Durrieu de Madron et al., 2005).

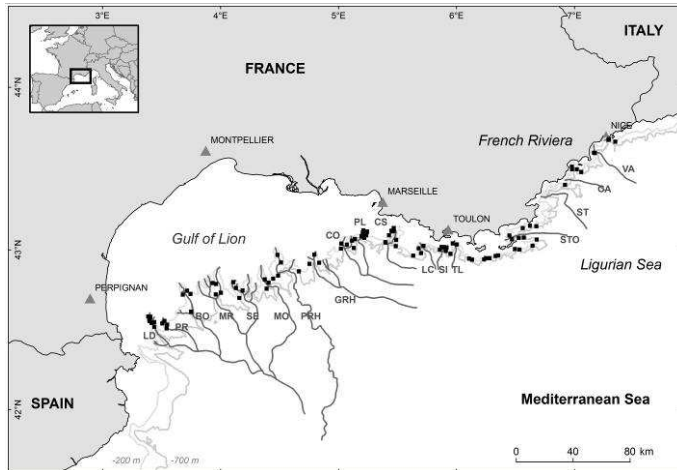


Fig. 1. The French continental margin of the Mediterranean Sea dissected by a series of submarine canyons.

From West to East: LD: Lacaze-Duthiers, PR: Pruvost, BO: Bourcart (Aude), MR: Marti (Hérault), SE: Sète, MO: Montpellier, PRH: Petit Rhône, GRH: Grand Rhône, CO: Couronne, PL: Planier, CS: Cassidaigne, LC: La Ciotat, SI: Sicié, TL: Toulon, STO: Stoechades, ST: Saint-Tropez (not considered in this study), CA: Cannes, VA: Var. Black squares represent the dives considered in this study (> 180 m depth) during the MEDSEACAN 2009, MARUM 2009, MARUM-Senckenberg 2011, ESSROV 2010 and CYATOX 1995 cruises.

2.2 Data origin

2.2.1 New data

Recent data were collected during the MEDSEACAN cruise organised by the “Agence des aires marines protégées” (Aamp) in 2009. The aim of the cruise was to explore the head of the canyons and so it was not specifically dedicated to the census of Vulnerable Marine Species. The data obtained from a total of 101 dives performed with the ‘Super Achille’ Remotely Operated Vehicle (ROV) from Comex (www.comex.com) are used for this paper (Table 1). The manned submersible ‘Remora’ was also deployed during the MEDSEACAN cruise, but the video films taken were not processed for this study, apart from one taken during a dive in the Bourcart canyon (BO_R2K_P1). Seventeen submarine canyons dissecting the French continental slope in the Mediterranean Sea, and the open slope between the Toulon and Stoechades canyons were explored in the bathyal bathymetric zone, from 180 to 700 meters depth (Fig. 1).

Additional video films were collected during two other cruises with the Comex team: the 2009 MARUM cruise (R/V “Minibex”; P.I. D. Hebbeln) to the Cassidaigne canyon and the 2011 MARUM-Senckenberg cruise (R/V “Minibex”; P.I. S. Tesche) to the Lacaze-Duthiers canyon (Table 2). The ‘Super Achille’ ROV and the manned submersible ‘Remora’ were deployed to collect colour video films and digital images and, exceptionally, a few samples. Data from four more dives were processed qualitatively: one dive with the Ifremer manned submersible Cyana (dive 1214-03 during the cruise CYATOX in 1995 (R/V “Le Suroit”; P.I. F. Galgani) and three dives (397-01, 401-05, 407-11) with the Ifremer Victor 6000 ROV from cruise ESSROV in 2010 (R/V “Pourquoi Pas?”; P.I. P. Simeoni) (Table 2). The global bathymetric map (100 m grid) of the French Mediterranean coast was compiled at Ifremer from different cruises (Loubrieu and Satra, 2010). The detailed bathymetric map (10 m grid) of the Bourcart canyon was obtained from the Marion 2000 cruise (Berné, 2000).

2.2.2 Historical data

Distribution maps of several Vulnerable Marine Ecosystems were digitalized from old documents in order to complete the information gathered from submersible exploration. The

207 distribution of *Isidella elongata* and *Funiculina quadrangularis* were assessed previously in the Gulf
208 of Lion and in the Ligurian Sea by trawling (Carpine, 1964; Fredj, 1964; Maurin, 1962).

209

210 2.3 *Processing of video and navigation data*

211

212 The exploratory dives were performed by the ROV equipped with two cameras. One was fixed
213 to a pan and tilt mount used by the pilots and recorded continuously on DVcam tapes and a hard disk
214 recorder. The other was fixed and mounted under the first one. This camera was equipped with a zoom
215 and could record HD images and HD video, but not continuously. The ROV navigation data were
216 derived from the SSBL subsea positioning system, Kongsberg HPR 410, and the surface positioning
217 system, DGPS AG132 – Trimble and Vector – Hemisphere GPS.

218 The distribution of communities, species and other objects and features (e.g. litter and fishing
219 impacts) was mapped along dive tracks from video studies of each dive, using the Ifremer underwater
220 vehicle data post-processing software "Adelie" (www.ifremer.fr/adelie) including an extension for the
221 ArcGIS 9.3 software suite (© ESRI). The navigation files included date, time, latitude, longitude,
222 heading and depth. All the Super Achille navigation track data had to be formatted manually in order
223 to enter the dedicated Ifremer "Adelie" extension. The navigation data were post-processed using
224 Gaussian smoothing. For the sake of practicality, the video films (10 minutes each) from the
225 MEDSEACAN cruise were concatenated and encapsulated in order to obtain one video film
226 corresponding to one dive to facilitate handling. Metadata from images captured during the Super
227 Achille dives, like date, time and image name, were grouped manually in a distinct file in order to
228 georeference these images via time codes within ArcGIS. Certain digital images were captured
229 directly on board in real-time during the Super Achille dives. In addition, georeferenced minifilms
230 were extracted with a 2 second image interval from the video films of the 2009 MARUM cruise and
231 the 2011 MARUM-Senckenberg cruise. "Adelie" also allowed us to complete this image collection
232 with georeferenced still images from the video films. The Geodesic system used was WGS84, in
233 Mercator projection with standard parallel N42.

234 In this paper we focused on the occurrences of benthic fishes, Vulnerable Marine Ecosystems,
235 and anthropogenic impacts located deeper than 180 m. Dive navigation tracks that occurred above 180
236 m depth were not considered.

237

238 2.4 *Distribution of benthic megafauna species*

239

240 In order to estimate abundances along navigation tracks each individual and colony record was
241 plotted on the GIS and represented by a point. A video still of every record was captured and geo-
242 referenced in a GIS when no digital image was available. Every specimen was identified at the lowest
243 possible taxonomic level. However, identification at species level for some organisms from video
244 footage was sometimes hampered due to poor video quality, high particle content in the water column
245 and/or limited resolution for detecting morphological characteristics distinguishing similar species and
246 had to be based on sampling. J. Vacelet (Marseille Univ.) assisted with Porifera identification,
247 S. Sartoretto (Ifremer Toulon) and H. Zibrowius (Marseille) with cnidarian identification, E. Gramitto
248 (ISMAR-CNR) with Actinopterygii Ophidiiformes identification, A. Souplet with Caridea
249 identification and S. Iglesias (MNHN Paris) assisted with Actinopterygii identification.

250

251 2.5 *Distribution of substrates*

252

253 Two types of substrates could be seen in the video films: soft substrates and hard substrates.
254 They were mapped along navigation tracks and the percentage per dive was calculated.

255

256 2.6 *Distribution of bauxite red mud deposition*

257

258 Every occurrence of red mud observed in the video films recorded in the Cassidaigne canyon
259 was georeferenced and mapped.

260

261 2.7 *Distribution of anthropogenic litter*

262
263
264
265
266
267
268
269
270
271
272
273
274
275
276
277
278
279
280
281
282
283
284
285
286
287
288
289
290
291
292
293
294
295
296
297
298
299
300
301
302
303
304
305
306
307
308
309
310
311
312
313
314
315
316

In order to estimate abundances along navigation tracks, we focused on plotting occurrences of anthropogenic litter. They were classified into seven classes (metal, glass, plastic, pottery, wood, concrete, others - including fabric and paper-board) according to the method described previously (Spengler and Costa, 2008).

2.8 Quantification and distribution of trawling impacts and lost fishing gears

Trawling scars were counted along the navigation tracks when they were isolated and considered to be at least one meter in width. When they covered a large part of the navigation track with no possible individualization, the length of the disturbance was measured along the navigation track. Both types of trawling scar lengths were totalled and the percentage of the disturbance was calculated with regard to the total navigation track length of the dive. Lost fishing gears observed along navigation tracks were quantified and georeferenced.

2.9 Abundances ($occurrence.km^{-1}$)

Evaluating surface areas and thus fauna densities from the video films was not possible technically, since: (1) the parameters (zoom, pan and tilt) of the camera used to record continuously were not steady; (2) the absence of lasers on the continuously recorded camera prevented the calculation of surfaces. In addition to these technical problems, the exploratory nature of the dives inevitably influenced the navigation tracks, introducing a bias in the data. Indeed, pilots and scientists tended to follow topographic features associated with fauna, which is completely different from following a pre-determined transect dedicated to the objective sub-sampling of spatial data.

With regard to these difficulties we decided not to calculate densities but to estimate abundances along navigation tracks. Event records per dive were extracted from the GIS distribution tables and their abundance was then standardized by dividing the counts by the length of the navigation track (calculated with the GIS tools). Each abundance was then calculated as a function of a one kilometer navigation track.

2.10 Abiotic parameters

The length of dive tracks was calculated using the Spatial Analyst Tool from ESRI GIS. Min. and Max. depths were extracted from navigation files or read on the video records when not available or incorrect in the navigation files.

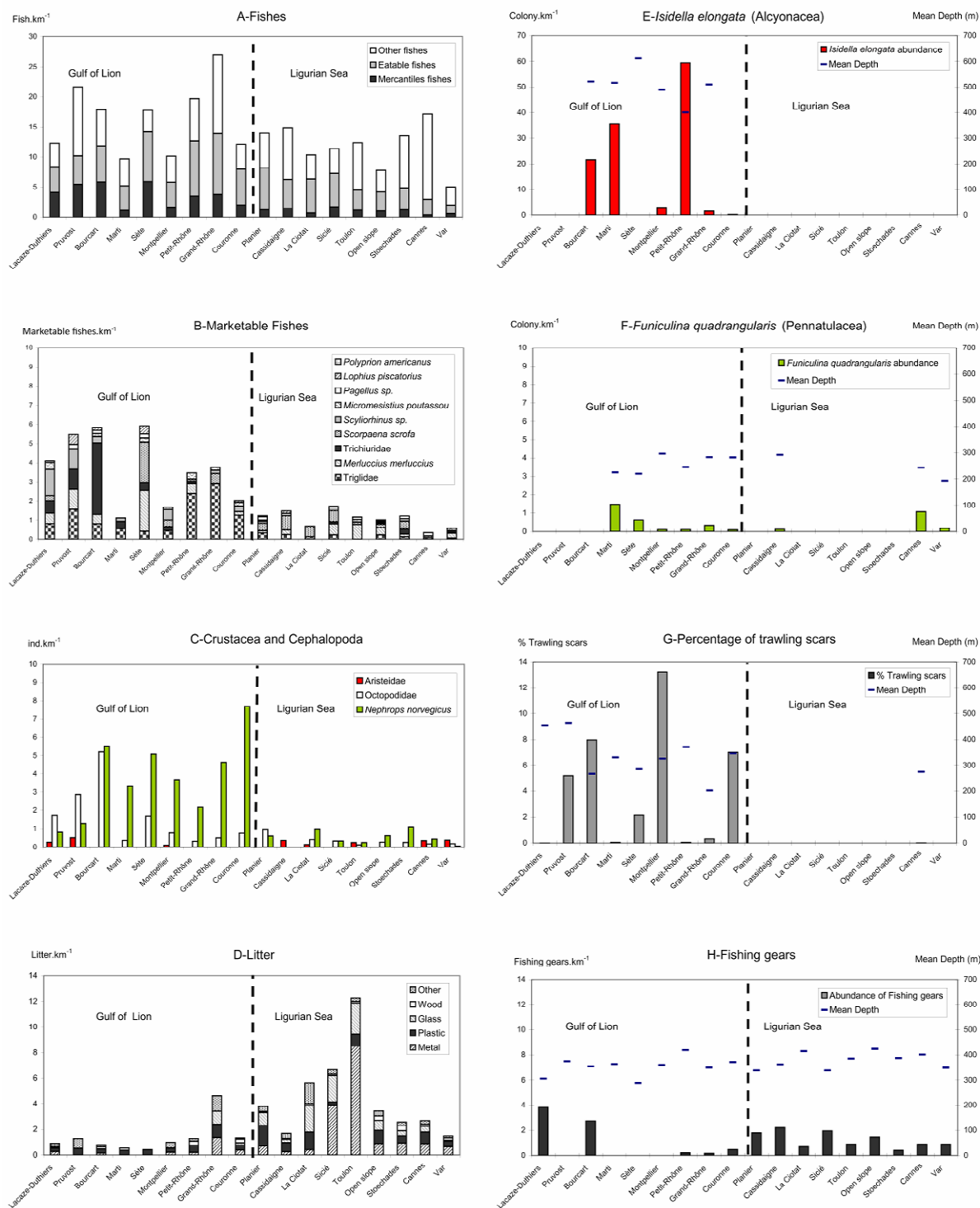
The Euclidian distance to the coast was calculated in three steps. Firstly, each navigation track was reduced to its centre of gravity. The raster of the Euclidian distance to the closest coast line was generated and converted into a point shapefile. A spatial join between the two shapefiles (navigation track and distance to the closest coast) allowed calculating the distance to the closest coast for each navigation track.

The mean slopes for every navigation track were calculated in degrees from 0 to 90. A raster of the slopes was produced from the compiled bathymetry (100 m grid) of the Mediterranean Sea (Loubrieu and Satra, 2010). Polygons were created for each navigation track line using 70 m width buffers and converted into a raster shape file. A zonal statistics table generated by the Spatial Analyst Tool allowed summarising the mean slope values within the zone of another dataset, in our case the navigation track polygons.

2.11 Statistical analyses

Biogeographical analyses were performed on VME fauna and resource abundances averaged per canyon. Cluster analysis, non-metric Multi-Dimensional Scaling (nMDS) and Principal Component Analyses (PCA) were performed using PRIMER (Plymouth Routines in Multivariate Ecological Research, Ver. 5, (Clarke and Warwick, 2001)). Vertical distribution box plots and student t-tests were performed using R freeware.

317 We used Redundancy Analysis (RDA) in a multiple linear regression procedure in order to
 318 understand the effect of depth, slope and distance to the coast on the distribution of litter between
 319 canyons. RDA uses permutation testing to find the significance of explained variation (R freeware).
 320



321
 322 **Fig. 2:** Histograms of abundances.
 323 Selected taxa, litter and fishing impacts observed in the French canyons are shown from west
 324 to east.
 325

326
327
328
329
330
331
332
333
334
335
336
337
338
339
340
341
342
343
344
345
346
347
348
349
350
351
352
353
354
355
356
357
358
359
360
361
362
363
364
365
366
367
368
369
370
371
372
373
374
375
376
377
378
379
380

3. Results

3.1 Distribution of fishing resources

3.1.1 Distribution and abundance of fishes observed on the seafloor

The fish species observed on the video films recorded along dive navigation tracks were listed with their abundance and maximum depth (Table 3). At least 59 mainly benthic and demersal species were recognized.

The most abundant species was *Helicolenus dactylopterus*, which was also the only species observed in every canyon. Two species were observed in shoals, *Trachurus* sp. and *Anthias anthias*, which were not counted and therefore removed from the following analyses. The other abundant species (>50 records for 101 dives) were *Coelorinchus caelorhincus*, *Phycis blennoides*, *Gadiculus argenteus*, *Capros aper*, *Galeus melastomus*, *Trigla lyra*, *Merluccius merluccius*, *Argentina sphyraena*, *Lepidorhombus boscii*, and *Scorpaena scrofa*.

Co-occurrences of fish species with vulnerable sessile marine species such as *Anthias anthias* were observed in shoals around bushes of *Madrepora oculata* in the Cassidaigne canyon, and *Benthocometes robustus* was observed only in the close vicinity of large colonies of gorgonians (*Callogorgia verticillata*) and antipatharians (*Leiopathes glaberrima* and *Antipathes* cf. *dichotoma*) up to 1 meter long in the Bourcart and Cassidaigne canyons.

The benthic fishes observed in the video films were classified into three categories: Marketable (M), Edible (E) and Others (O) (Table 3). Their abundance and distribution between canyons is presented in Fig. 2A. The distribution of marketable benthic fishes was analyzed in more detail as they are targeted by fisheries and their presence leads to impacts on the bottom caused by fishing.

3.1.2 Distribution and abundance of marketable benthic fishes

Of the 13 marketable fish species mentioned in table 3, we kept only 9 for the analysis. *Trachurus* sp. and *Zeus faber* were removed because one is pelagic and the other is from the shelf. *Scyliorhinus canicula* and *Scyliorhinus* sp. were grouped into *Scyliorhinus* spp. *Trigla lyra* and Triglidae were grouped into Triglidae. The 9 marketable fishes considered in the study are therefore *Lophius piscatorius*, *Merluccius merluccius*, *Micromesistius poutassou*, *Pagellus* sp., *Polyprion americanus*, *Scorpaena scrofa*, *Scyliorhinus* sp., Trichiuridae and Triglidae.

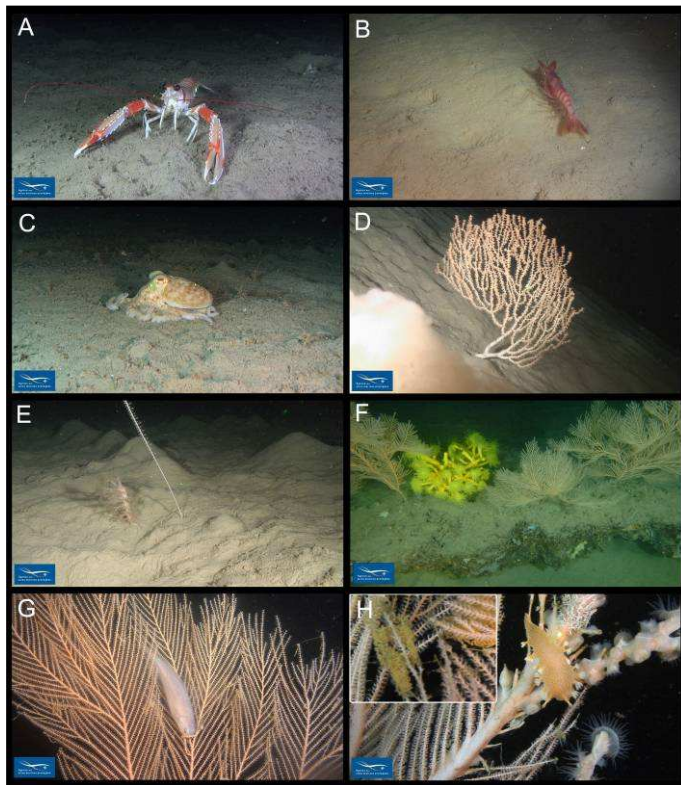
Triglidae were the most abundant, followed by *Merluccius merluccius*, Trichiuridae and *Scorpaena scrofa*. The Gulf of Lion (from Lacaze-Duthiers to Couronne) presents higher abundances of these marketable fishes than the Ligurian Sea (Student test, $p < 0.0005$, variance equality), with two exceptions: the Marti and Montpellier canyons in which we observed fewer fishes (Fig. 2B).

3.1.3 Crustacea and Cephalopoda: *Nephrops norvegicus*, Aristeidae and Octopodidae

Nephrops norvegicus, a commercial crustacean, was found in every canyon explored apart from the Cassidaigne canyon (Fig. 2C). They were always observed defending their burrows against the ROV (Fig. 3A). The highest abundances were recorded in the Gulf of Lion in the Couronne canyon and Bourcart canyon. A total of 286 individuals were counted. They were located at a mean depth of 380 m (+/- 51 m).

Aristeidae, or red shrimps, were rarely observed in the videos (Fig. 3B). A total of 22 individuals were counted (Fig. 2C). They were located at a mean depth of 542 m (+/- 104 m). Shrimps of the Pandalidae family could be observed in higher abundance than Aristeidae, but they are not targeted by fisheries and are bycatch species.

Octopodidae were much more frequent in the Gulf of Lion than in the Ligurian Sea (Fig. 2C). The highest abundance was recorded in the Bourcart canyon. A total of 150 individuals were observed. They were located at a mean depth of 330 m (+/- 81 m). Some individuals were very small, only 7 cm (Fig. 3C).



381
 382 **Fig. 3:** MEDSEACAN cruise images of commercial resources and vulnerable marine species.
 383 **A:** *Nephrops norvegicus* on bathyal bioturbated mud in the Planier canyon, dive P10, 395 m.
 384 **B:** A red shrimp, *Aristeus antennatus*, on bathyal mud in the Lacaze-Duthiers canyon, dive
 385 P13, 663 m. **C:** An example of *Octopodidae* on bathyal mud in the Couronne canyon, dive P1,
 386 226 m. **D:** *Isidella elongata* on a sloping seafloor of compact mud in the Montpellier canyon,
 387 dive P3, 573 m. **E:** *Funiculina quadrangularis* (right) and *Kophobelemnion leucharti* (left) on
 388 bioturbated soft mud in the Marti canyon, dive P4, 227 m. **F:** Large colonies of *Callogorgia*
 389 *verticillata* and *Dendrophyllia cornigera* on a rocky slab in the Boucart canyon, dive
 390 BO_R2K_P1, 350 m. **G:** The *Ophiidiidae* *Benthocometes robustus* hiding in a *C. verticillata*
 391 colony in the Bourcart canyon, dive BO_R2K_P1, 350 m. **H:** *Nudibranchia Tritoniidae* and the
 392 parasitic zoanthid *Isozoanthus primnoidus* living on a colony of *C. verticillata*; insert: detail of
 393 *Tritoniidae* eggs in the Sicié Canyon, dive P4, 261 m.

394
 395
 396

397 3.2 Distribution of Vulnerable Marine Ecosystems

398

399 3.2.1 Distribution and abundance of *Isidella elongata* communities observed on bathyal mud

400

401 *Isidella elongata* colonies were observed in the Gulf of Lion during the MEDSEACAN cruise.
 402 They were found in higher abundance in three canyons: Bourcart (dive P5), Marti (P1 and P5), and
 403 Petit-Rhône (P3, P4 and P5) (Fig. 2E). A total of 913 colonies were counted. They were located at a
 404 mean depth of 459 m (+/- 84 m).

405

406 In the Bourcart canyon, colonies were observed between two gullies on the west flank (P5),
 407 with equal proportions of small (10/20 cm) and medium/large (40/60 cm) colonies. Trawling scars
 408 were also seen in this canyon, located on the other flank (P6).

409

410 In the two other canyons (Marti and Petit-Rhône) no trawling scars were seen where two
 411 meadows of *I. elongata* were present on sloping seafloor (about 10 to 20°) (Greene and Bizzarro,
 2007). In the Marti canyon, all the colonies were small (20 to 30 cm high), while in the Petit-Rhône
 canyon (P5) large (60 cm) and small colonies (10/20 cm) could be observed close together, standing
 and healthy (Fig. 3D).

412 A few other colonies were observed in lower abundance in four canyons: Montpellier, Grand-
 413 Rhône, Couronne and Cassidaigne (one live colony and three dead ones in upright position, smothered
 414 with the red mud, MARUM 2009 cruise, dive D3).

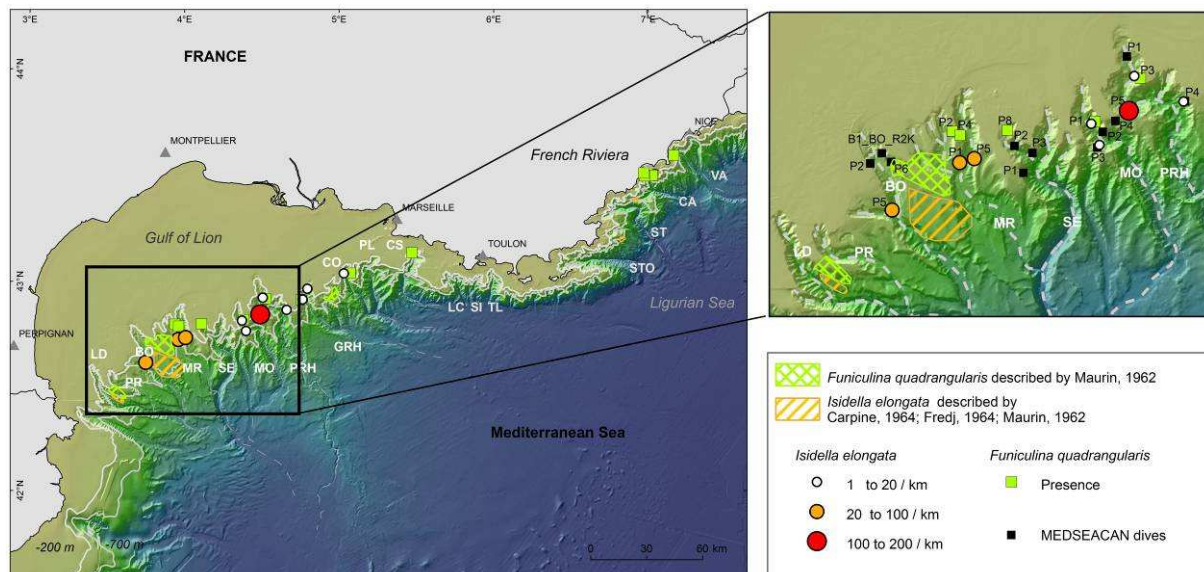
415 The mud on which *I. elongata* colonies were established presented small domes or tumuli and
 416 holes, indicating a high level of bioturbation, mainly due to crustaceans. Many of these could be seen
 417 in the videos, including some Galathea (*Munida* sp.), Caridea (*Plesionika* sp.) and Axiidea
 418 (*Calocaris macandreae*), though the majority was made up of Nephropidae (*Nephrops norvegicus*). *I.*
 419 *elongata* was usually located on sloping seafloors (about 10 to 20°).

420

421 3.2.2 Distribution of *Funiculina quadrangularis* communities on bathyal mud

422 The highest abundance of *F. quadrangularis* was observed in the Marti canyon and in the
 423 Cannes canyon (Fig. 2F). A total of 32 colonies were observed at a mean depth of 239 m (+/- 31 m).

424



425

426 **Fig. 4:** Distribution of *Isidella elongata* and *Funiculina quadrangularis* observed during the
 427 MEDSEACAN dives in French canyons and as described by Maurin, 1962, Carpine, 1964 and
 428 Fredj, 1964.

429 Submarine canyons from West to East: LD: Lacaze-Duthiers, PR: Pruvost, BO: Bourcart
 430 (Aude), MR: Marti (Hérault), SE: Sète, MO: Montpellier, PRH: Petit Rhône, GRH: Grand Rhône,
 431 CO: Couronne, PL: Planier, CS: Cassidaigne, LC: La Ciotat, SI: Sicié, TL: Toulon, STO:
 432 Stoechades, ST: Saint-Tropez (not considered in this study), CA: Cannes, VA: Var.

433

434

435 3.2.5 Distribution of *Callogorgia verticillata* communities observed on hard substratum

436 The highest abundance was found in the Bourcart canyon (Dive _R2K_P1), followed by the
 437 Cassidaigne (P7, MARUM D2, D9), Planier (P8 and P11), Sicié (P4), Toulon (P4 and P5) canyons
 438 and on the open slope between Toulon and Stoechades (PO_P5) (Fig. 5). A total of 452 colonies were
 439 observed at a mean depth of 360 m (+/- 60 m).

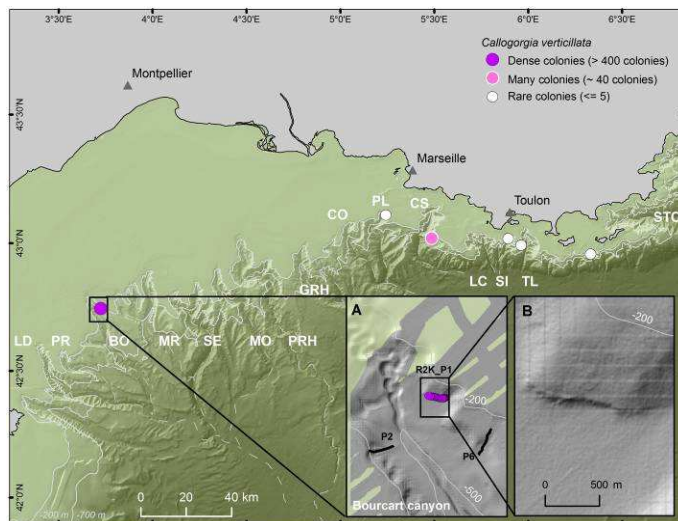
440 In the Bourcart canyon we observed an exceptionally high density of the Primnoidea *C.*
 441 *verticillata* (Fig. 3F). The colonies were encountered on the eastern flank of the canyon, during the
 442 MEDSEACAN cruise dive BO_R2K_P1. About 400 colonies were seen forming a 900 meter line
 443 along a cornice. They were recorded by video (Fig. 5A). The cornice was a slab of hard substratum
 444 located at a depth of 350 m (Fig. 5B). The fan-shaped colonies were up to one meter in height and
 445 oriented perpendicular to the slope. They sheltered a high diversity of megafauna including: Porifera,
 446 Scleractinia (*Dendrophyllia cornigera*, *Desmophyllum dianthus* and *Madrepora oculata*), Antipatharia
 447 (*Leiopathes glaberrima* and *Antipathes* sp.), Echinodermata (*Cidaris cidaris*, *Echinus melo* and
 448 *Echinus* sp.), Crustacea (lobster *Palinurus mauritanicus*, Caridea *Plesionika* sp. and Galatheaidea),
 449 Mollusca (Octopodidae), Actinopterygii (*Phycis blennoides*, *Phycis phycis*, *Lophius piscatorius*,

450 *Helicolenus dactylopterus*, *Conger conger*, *Benthocometes robustus* and Trichiuridae), and
451 Holocephali Chimaeridae (*Chimaera monstrosa*). Three individuals of the Actinopterygii
452 *Benthocometes robustus* were observed hiding in *C. verticillata* fans with their heads pointing
453 downwards (Fig. 3G). Evidence of fishing disturbance was observed many times with bottom lines
454 and fishing nets hooked onto the hard cornice and damaging colonies of *C. verticillata*.

455 The Cassidaigne canyon is a semi-enclosed basin. Outside this basin, facing the abyssal plain on
456 the open slope, a field of *C. verticillata* (43 colonies) was encountered during dive P7 (Fig. 5). The
457 colonies, found at a depth from 390 to 350 m, were separated from each other by a distance from 3 to
458 4 meters. Dispersed colonies were also frequently encountered at depths of 200-294 m, specifically on
459 rocky outcrops along spurs of the western flank of the Cassidaigne canyon (MARUM 2009 cruise,
460 dives D2 and D9). Some live branches of a *C. verticillata* colony were covered by ophiuroids and
461 crinoids, whereas on the basal stem, large aggregations of the serpulid *Filograna* sp. and sponges were
462 present.

463 Few *C. verticillata* colonies were encountered in three other canyons (Planier, Sicié and Toulon)
464 and on the open slope between Toulon and Stoehades, and always on raised slabs. Colonies were one
465 to two meters high and accompanied by several species: pagurids, a comatulid crinoid (*Antedon* sp.),
466 *Scorpaena scrofa*, a cnidarian (*Gerardia* sp.), a zoantharian (*Isozoanthus primnoidus*), and a tritoniid
467 nudibranch that had laid its eggs on a gorgonian (see Fig. 3H).

468



469

470 **Fig. 5.** Spatial distribution of *Callogorgia verticillata* observed during the MEDSEACAN cruise.

471 **A:** Zoom on the Bourcart canyon where dive BO_R2K_P1 took place. **B:** Zoom on the 900 m

472 long cornice of hard substratum in the Bourcart canyon (350 m depth) where colonies of *C.*

473 *verticillata* were aligned (see Fig. 3F).

474

475

476

477 3.2.6 Distribution of cold-water coral communities observed on hard substratum

478 In the Mediterranean deep-sea two scleractinian species, *Lophelia pertusa* and *Madrepora*
479 *oculata*, make up the dominant structure-forming corals (Fig. 6A).

480 The Lacaze-Duthiers canyon is the only French Mediterranean canyon where the two species *L.*
481 *pertusa* and *M. oculata* have been observed living together in large quantities, the situation generally
482 described for the biocoenosis of cold-water corals (CWC). In this canyon large colonies (> 40 cm) of
483 both species of scleractinians were observed at depths ranging from 246 m to 541 m at the head of the
484 canyon and its western flank during the MEDSEACAN and MARUM-Senckenberg 2011 cruises (Fig.
485 7A). This canyon was highly loaded in particles, making it difficult to analyse the video films.

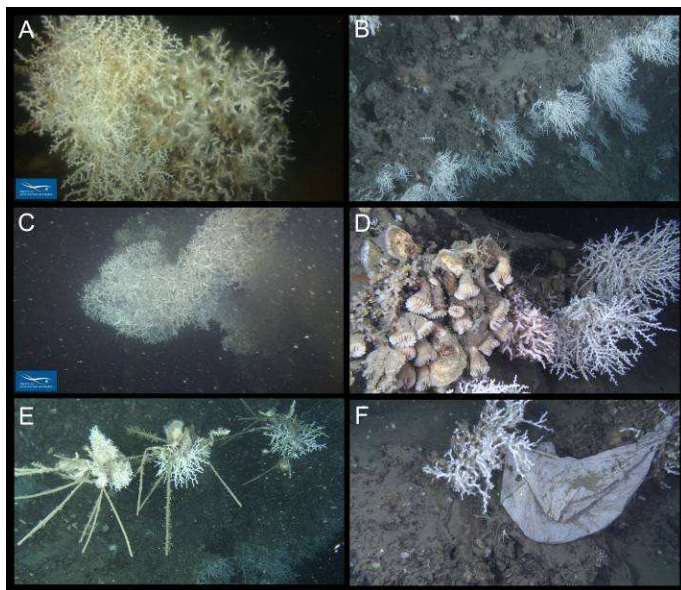
486 On the western flank of the canyon the two species of scleractinians were observed during dives
487 P15, D2, D6 and D7 aligned on edges at depths between 340 and 350 m. During dive P15, this edge
488 was followed along an 800 m long navigation track and revealed medium-sized (20 to 40-cm in
489 length), downward-growing colonies of *L. pertusa* and *M. oculata* (Fig. 6B). Toward the end of the

490 dive, we encountered large (> 50 cm), healthy bushes of *L. pertusa* (Fig. 6C) covering an overhanging
 491 wall 10 m high and 20 m wide at 330 m depth on the western flank of the canyon (42°33.677' N,
 492 3°23.940' E), on which many medium-sized colonies (around 20 cm) of *M. oculata* co-occurred. A
 493 considerable amount of coral rubble was partially buried in the sediment lying at the bottom of this
 494 wall. *M. oculata* was observed without *L. pertusa* (dives P2, P11, P15 and D5) on the same flank at
 495 shallower depths ranging from 246 to 325 m. On the same flank large, isolated bushes (> 50 cm) of *L.*
 496 *pertusa* were observed at deeper depths ranging from 507 to 541 m during dive P6, while only a few
 497 isolated colonies of *M. oculata* were encountered from 376 to 531 m depth.

498 On the eastern flank of the canyon, during dive P3, another edge of hard substratum was
 499 followed along 400 m at about 260 m depth. This edge created an overhang under which a series of *M.*
 500 *oculata* colonies were aligned growing downward. Few *L. pertusa* colonies were observed on this
 501 flank (six colonies during dive P3 and one colony during dive P14) and they were partly covered with
 502 particles and epibionts. A large number of old fishing lines were tangled on the edge and in the CWC
 503 frameworks. The top of the edge was covered with a continuous layer of sediment.

504 A considerable diversity of CWC associated species could be seen (Fig. 6D) in the Lacaze-
 505 Duthiers canyon. The fishes observed were mainly Actinopterygii represented by Macrouridae
 506 (*Coelorinchus caelorhincus*), Moridae (*Phycis blennoides*), Scorpaenidae (*Helicolenus dactylopterus*)
 507 and Trichiuridae. Some Elasmobranchii were also present with Carchariniformes (*Scyliorhinus*
 508 *canicula*) and Squaliformes (*Oxynotus centrina*). Echinoidea (*Cidaris cidaris*, *Echinus melo*,
 509 *Gracilechinus acutus*), Scleractinia (*Desmophyllum dianthus*, *Dendrophyllia cornigera*), Bivalvia
 510 (*Neopycnodonte cochlear*), Porifera (*Poecillastra compressa*, *Hamacantha falcula*, and others),
 511 Crustacea (Paguroidea and Galatheididae) and Ascidiacea were numerous in these ecosystems. Some
 512 Comatulida (*Leptometra phalangium*) were observed on an old fishing line trapped on the bottom. No
 513 Antipatharia were observed during the dives carried out in the Lacaze-Duthiers canyon.

514



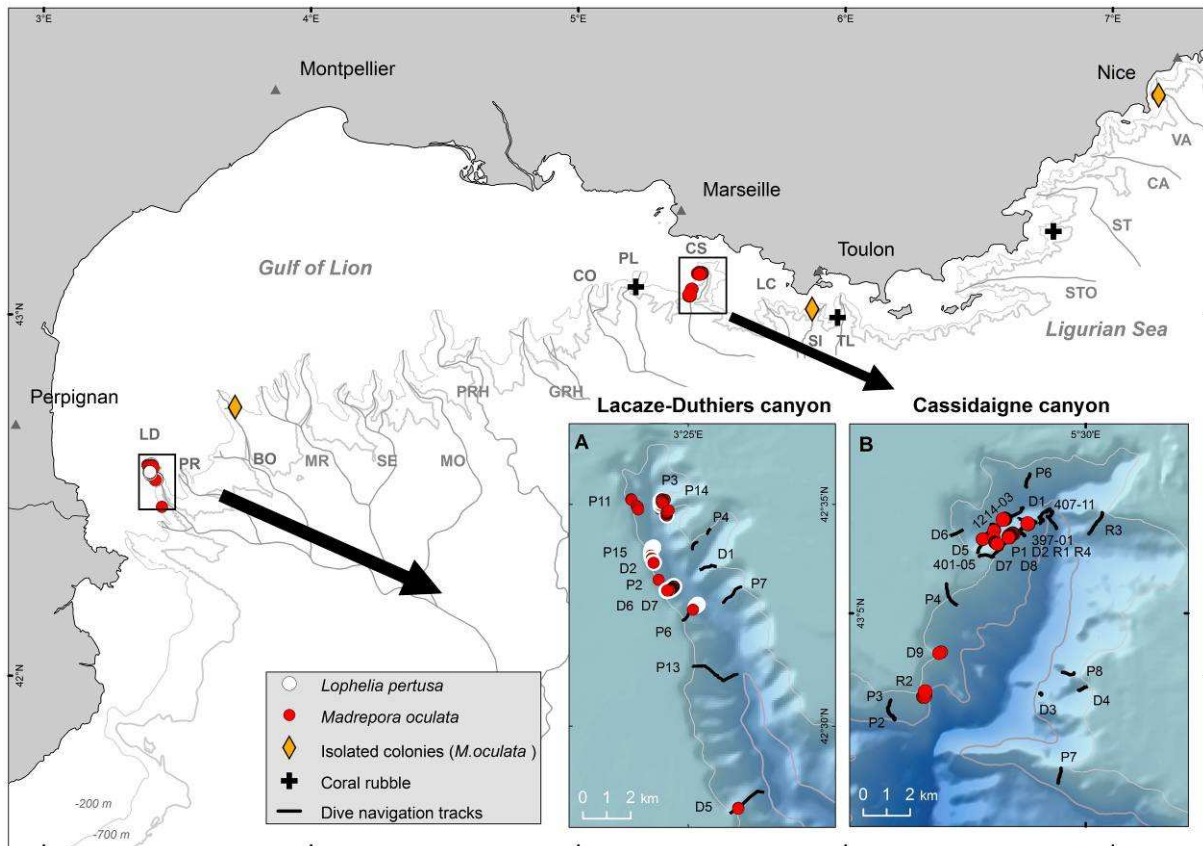
515

516 **Fig. 6.** Cold-water Corals in the Lacaze-Duthiers canyon.

517 **A:** Colonies of *Madrepora oculata* (left) and *Lophelia pertusa* (right), MEDSEACAN cruise ,
 518 dive P15, 369 m. **B:** Colonies of *M. oculata* growing downward, MARUM-Senckenberg cruise,
 519 dive D7, 342 m. **C:** Large colonies of *L. pertusa* covering a vertical cliff and growing
 520 horizontally, MEDSEACAN cruise, dive P15, 343 m. **D:** Communities of *M. oculata* and *L.*
 521 *pertusa* colonies together with *Desmophyllum dianthus* and *Neopycnodonte cochlear*
 522 specimens, MARUM-Senckenberg cruise, dive D6, 387 m. **E:** Lost long line under tension
 523 serving as substrate for sabellids, serpulids (amongst *Filograna* sp.), *L. pertusa* and
 524 *Neopycnodonte cochlear*, MARUM-Senckenberg cruise, dive D2, 331 m. **F:** Soft plastics
 525 entangled in *L. pertusa* causing necrosis in area of contact, MARUM-Senckenberg cruise, dive
 526 D6, 468 m.

527
528
529
530
531

The second CWC location in the area studied was the western flank of the Cassidaigne canyon. *M. oculata* seems to be the only structure-forming scleractinian as *L. pertusa* has never been recorded in this canyon.



532
533
534
535
536
537

Fig. 7: Distribution map of frame-building scleractinian cold-water coral communities. **A:** Zoom on the Lacaze-Duthiers canyon. **B:** Zoom in the Cassidaigne canyon.

538
539
540
541
542
543
544
545
546
547
548
549
550
551
552
553

The largest concentration of *M. oculata* colonies was observed on the west flank of the canyon along a crest (43° 06.76' N; 5° 27.62' E) during MEDSEACAN dive P1, MARUM 2009 dive D2, R1, R4 and ESSROV 2010 dive 401-05 at depths ranging from 200 to 210 m (Fig. 7B). At this location at the edge of the shelf, the velocity of the bottom current and the diversity were higher than what could be seen on the shelf above. The bedrock showed characteristic features of a formerly karstified landscape with dissolution holes forming cave galleries separated by pillars (Fig. 8A). The rugged topography of this karstified spur caused the loss of many fishing gears (Fig. 8B). Large bushes of *M. oculata* were observed covering the substratum whose relief was extremely rough below the overhangs (Fig. 8C). Mature *M. oculata* colonies attained heights up to 40 cm. *M. oculata* co-occurred with many Porifera (*Poecillastra compressa* and others that could not be identified on the video films), Antipatharia (*Leiopathes glaberrima*, *Antipathella subpinnata*, *Antipathes* cf. *dichotoma*), Scleractinia (*Dendrophyllia cornigera*), Alcyoniina (*Gersemia* sp.), Ophiuroidea (*Astrospartus mediterraneus*), Echinoidea (*Cidaris cidaris*, *Echinus melo*), Crustacea (Brachyura), Bivalvia (*Spondylus gussoni*) and Actinopterygii (*Anthias anthias*, *Conger conger*, *Helicolenus dactylopterus*). At this site at 210 m depth, *M. oculata* could be seen mixed with species from circalittoral depths, such as *Holaxonia* (*Eunicella cavolini*, *Paramuricea clavata*) and *Scleraxonia* (*Corallium rubrum*) (Figs. 8D and 8E).

554
555

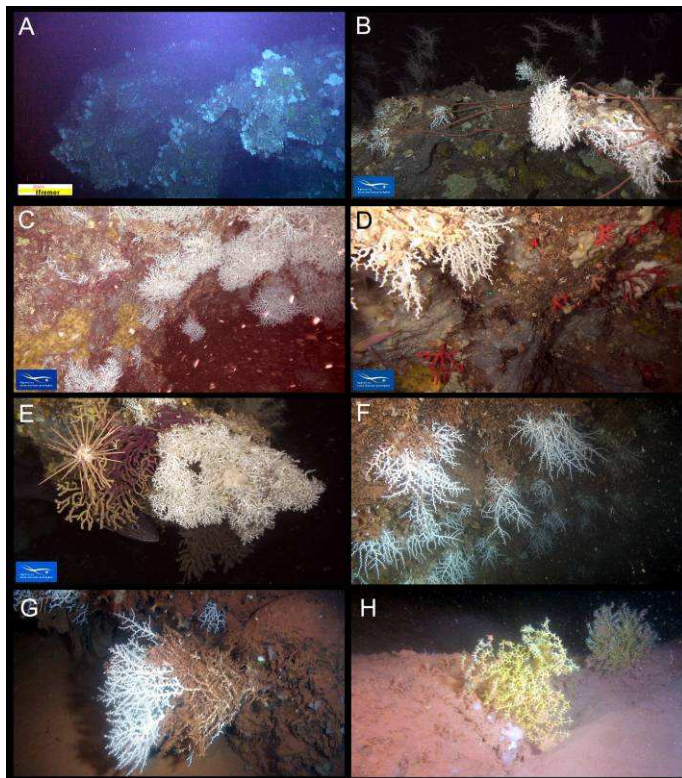
M. oculata could be observed in red mud below 350 m (see 3.3.6) (Table 1 and 2) on the north face of the edge during dives 1214-03, 397-01, D5, D7, D8 and R1.

556 Further south in the canyon, still on the west flank, a peculiar spot was discovered during dive
557 R2. This was a vertical escarpment descending from 320 m depth down to at least 480 m. The wall
558 was colonised locally by recently settled dense colonies of *M. oculata* with very fragile branches
559 hardly exceeding 4 cm in length. During dive D9, two small healthy colonies of *M. oculata* were
560 observed at 324 and 244 m depth fixed on a vertical wall on which could also be seen colonies of
561 *Leiopathes glaberrima* and *Corallium rubrum*.

562 The giant deep-sea oyster, *Neopycnodonte zibrowii*, was frequently encountered on (sub-)
563 vertical flanks and overhangs of bedrock exposed in the 376-470 m depth range and appeared to be
564 fossilised during dives D1, D7 and D9.

565 During the MEDSEACAN cruise, previously non reported occurrences of *M. oculata* were
566 observed in three other canyons: Bourcart, Sicié and Var (Fig. 7, orange diamonds). In the Bourcart
567 canyon, *M. oculata* was observed on a shelf of hard substratum at 331 m depth, during dive
568 BO_R2K_P1 (42°44.688 N, 3°42.953 E). Several single branches protruded from a slab. In the Sicié
569 canyon a 15-cm colony of *M. oculata* was observed at 255 m depth (43° 0.873 N, 5° 52.501 E) while
570 in the Var canyon, three young branches 2 cm long were seen growing at 350 m depth on a wall of
571 hard rock (43°35.868 N, 7°9.863 E).

572 Several broken fragments of dead cold-water corals, probably *M. oculata*, were seen in the
573 Planier canyon (Dive P3) (Fig. 7, black crosses) but could not be collected. They were located at the
574 bottom of a cliff.
575



576
577 **Fig. 8:** *Madrepora oculata* and red mud deposits in the Cassidaigne canyon.
578 **A:** Characteristic features of the bedrock covered with *M. oculata* colonies, ESSROV 2010
579 cruise, dive 401-05, 238 m. **B:** Lost fishing gears entangled with *M. oculata* bushes in the
580 Cassidaigne canyon, MEDSEACAN cruise, dive P1, 200 m. **C:** Several white bushes of *M.*
581 *oculata* growing downward from a rocky overhang, dive P1, 205 m. **D:** Red coral *Corallium*
582 *rubrum* colonies co-occurring with *M. oculata* colonies, MEDSEACAN cruise, dive P1, 210 m.
583 **E:** High species diversity associated with *M. oculata* colonies: *Cidaris cidaris*, *Paramuricea*
584 *clavata* and *Conger conger* hiding below a coral framework, MEDSEACAN cruise, dive P1,
585 205 m. **F:** *M. oculata* colonies with elongated shapes and thin axes regularly spaced on a wall
586 covered with red mud, MARUM 2009 cruise, Dive D5, 365 m. **G:** *M. oculata* colonies with

587 basal portions lacking coral tissue colonised by epibionts like hydrozoans and covered with
588 red mud, MARUM 2009 cruise, dive D7, 464 m. H: Fan-shaped current facing colonies of
589 *Acanthogorgia hirsuta* fixed on a rocky slab covered with red mud, MARUM 2009 cruise, Dive
590 D1, 470 m.

591
592

593 3.3 Distribution of Vulnerable Marine Ecosystem (VME) fauna and anthropogenic impacts

594

595 3.3.1 Distribution of trawling scars on bathyal mud

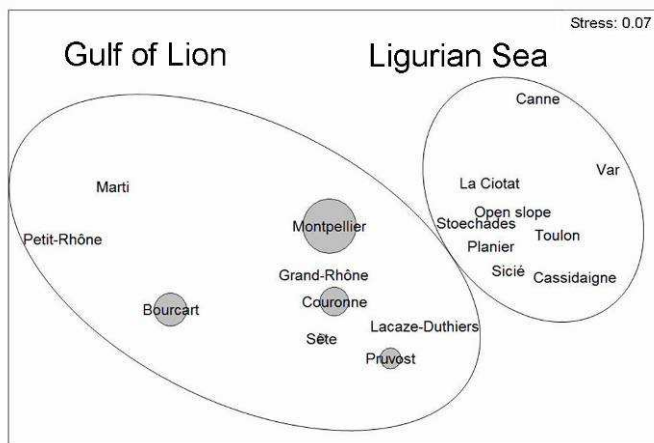
596 Trawling scars were mainly located in the Gulf of Lion (Fig. 2G). We observed some large
597 areas of sediment completely impacted (alternatively smoothed and ploughed) by repeated trawling in
598 five canyons: Pruvost, Bourcart, Sète, Montpellier and Couronne. A highly impacted area 800 m long
599 was observed in the Montpellier canyon, representing 43% of the navigation track (Fig. 13A).
600 Trawling scars were located at a mean depth of 330 m (+/- 64 m).

601

602 3.3.2 Analysis of the spatial distribution of resources and VME fauna on bathyal mud

603 The hierarchical classification of canyons with regards to their composition in resources
604 (marketable fishes, *Nephrops norvegicus*, Octopodidae) and VME fauna (*Funiculina quadrangularis*,
605 *Isidella elongata*) on bathyal mud shows that two groups of canyons are separated at a similarity
606 threshold of 45%: the Gulf of Lion and the Ligurian Sea.

607



608

609 **Fig. 9.** Non metric, multi-dimensional scaling ordination of canyons.

610 Bray-Curtis similarity coefficients of resources and VME fauna abundances were used for the
611 ordination. Clusters formed at the 45% similarity level and trawling impact represented by
612 circles of different sizes were superimposed on the MDS plot.

613

614

615 A non-metric, multidimensional scaling (nMDS) plot was produced by PRIMER (Fig. 9). A
616 stress value of 0.07 was derived by statistical processing, indicating good ordination. A cross-check
617 against the results of hierarchical classification was made by superimposing the groups having
618 similarities of 45%, corresponding to the Gulf of Lion and the Ligurian Sea. The superimposition of
619 trawling scar abundances highlights the fact that bottom trawling occurs only in the canyons of the
620 Gulf of Lion.

621

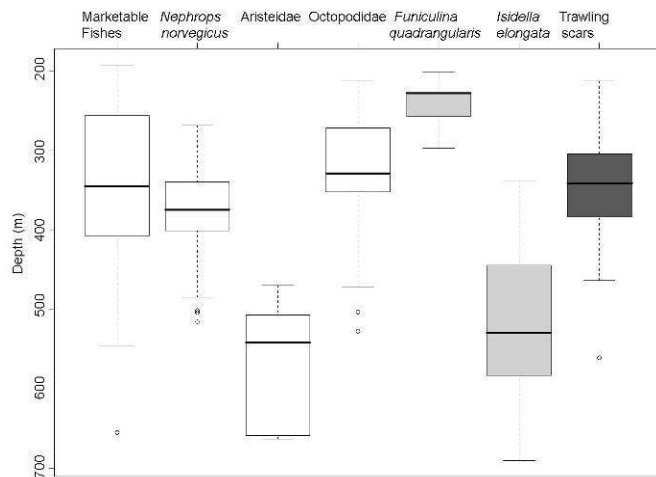
622 A Principal Component Analysis (PCA) was performed to ordinate canyons with regarding their
623 abiotic environmental parameters that had been normalised beforehand: percentage of mud and mean
624 slope encountered along navigation tracks. The first principal component axis explains 85% of the
variance between canyons and is driven by the percentage of mud.

625 The Gulf of Lion canyons are characterised by muddy substrates, while the Ligurian Sea canyons are
 626 characterised by hard substrates. The Lacaze-Duthiers canyon, which is in fact located in the Gulf of
 627 Lion, is represented in the Ligurian Sea canyons group, illustrating the high percentage of hard
 628 substrate in this canyon.

629

630 3.3.3 Vertical distribution of resources, VME fauna and the impact of trawling on bathyal mud

631



632

633 **Fig. 10.** Box-plot of vertical distributions in the Gulf of Lion.

634 Resources (white), VME fauna (light grey) and trawling impact (dark grey) observed on
 635 bathyal mud in the French canyons of the Gulf of Lion during the MEDSEACAN dives.

636

637

638 The vertical distribution of *Isidella elongata* and *Funiculina quadrangularis* was compared to the one
 639 of resources and trawling scars in the Gulf of Lion (Fig. 10). Specimens of *F. quadrangularis* were
 640 located at shallower depths (240 m) than trawling scars (355 m) whereas specimens of *I. elongata*
 641 were located at deeper depths (516 m) (Student tests show significant differences for both, $p < 0.05$).
 642 There was no statistical difference between depth of trawling scars and resources [marketable fishes
 643 ($p = 0.30$), *Nephrops norvegicus* ($p = 0.10$) and Octopodidae ($p = 0.36$)]. Aristeidae were located deeper
 644 (564 m), in the same range as *I. elongata* (516 m) (Student test show no significant difference,
 645 $p = 0.21$).

646

647

648 3.3.4 Distribution of lost fishing gears on hard substratum

649 Lost fishing gears could be observed in every canyon of the Ligurian Sea (from Planier to Var
 650 canyons) and in five canyons of the Gulf of Lion (Fig. 2H). They consisted of lost nets, lead weights
 651 and ropes, damaging structure-forming fauna and breaking cnidarian colonies. Long lines were often
 652 entangled around rocky obstacles and under tension. They formed an artificial substrate which was
 653 preferentially colonised by sabellid and serpulid polychaetes, and occasionally by *Neopycnodonte*
 654 *cochlear* and scleractinian corals (Fig. 6E). The highest abundances were recorded in the Lacaze-
 655 Duthiers, Bourcart (Fig. 2H) and Cassidaigne canyons (Fig. 13B). A total of 199 lost fishing gears
 656 were counted at a mean depth of 343 m (± 88 m).

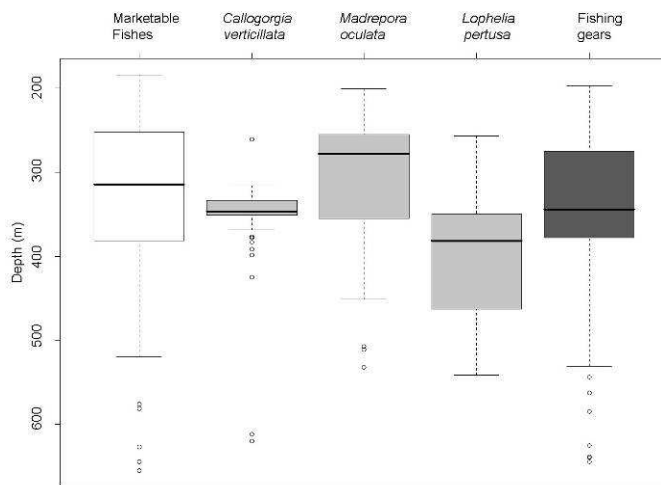
657

658

659 3.3.5 Analysis of the vertical distribution of VME fauna and lost fishing gears on hard substratum

660 The vertical distribution of *Callogorgia verticillata*, *Lophelia pertusa* and *Madrepora oculata*
 661 was compared to that of marketable fishes and fishing gears in the Lacaze-Duthiers, Bourcart and
 662 Cassidaigne canyons (Fig. 11). *C. verticillata* was located within a very narrow depth range around
 663 340 m. *L. pertusa* was found deeper than *M. oculata* (the Student test shows significant difference,

664 p<0.05). There was no statistical difference between depth of fishing gears and marketable fishes
 665 (p=0.11) or *C. verticillata* (p<0.05). On the contrary, fishing gears, *L. pertusa* and *M. oculata* were
 666 found at different mean depths (Student tests show significant differences, p<0.05), but their
 667 bathymetric ranges overlapped.
 668



669 **Fig. 11.** Box-plot of vertical distributions in the Lacaze-Duthiers, Bourcart and Cassidaigne
 670 canyons.
 671

672 Resources (white), VME fauna (light grey) and fishing gears (dark grey) observed during the
 673 MEDSEACAN dives on hard substratum in the Lacaze-Duthiers, Bourcart and Cassidaigne
 674 canyons.
 675
 676

677 3.3.6 Distribution of cold-water coral and bauxite red mud deposits in the Cassidaigne canyon

678 During all the dives in the north of the Cassidaigne canyon we observed a continuous thick
 679 layer of red mud below 350 m depth (Fig. 12). In the area affected by the red mud, *Madrepora oculata*
 680 was present in water depths from 365 to 515 m depth (dives D5, D7, 397-01 and 1214-03).

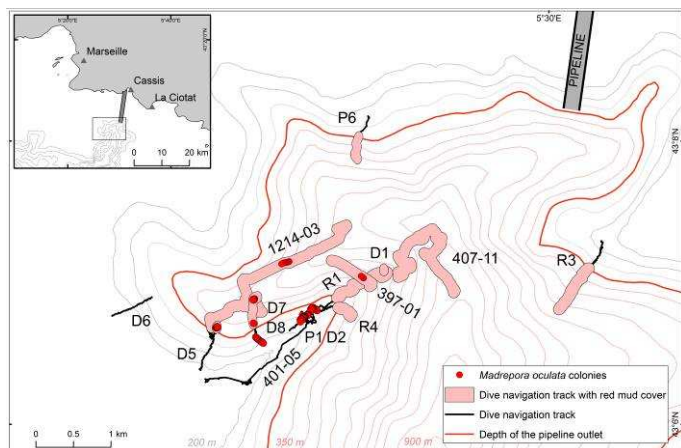
681 Dense bushes of *M. oculata* were recorded between 515 and 485 m depth (dive 1214-03) (Fig.
 682 12) on a vertical cliff in the northern part of the western gully. A large overhang at the summit of the
 683 cliff (5 m wide) was covered with red mud. The Cyana submersible followed the edge of the overhang
 684 for 10 minutes and dense bushes of *M. oculata* could be observed growing from the edge.

685 In the western gully, *M. oculata* could be observed (D5) at 365 m depth on a vertical wall 5 m
 686 high, slightly covered with red mud. The colonies on this wall were regularly spaced, had elongated
 687 shapes with thin axes (Fig. 8F) and grew horizontally or downwards. They seemed to have settled
 688 recently. A dozen white colonies were also observed on a small rocky slab completely covered with
 689 red mud at 466 m depth (D7) (Fig. 8G).

690 Along the rocky edge at depths ranging from 300 to 390 m, sparse bunches of *M. oculata* were
 691 recorded on small rocks emerging from the substrate covered with red mud (dives 397-01 and R1).

692 Below 350 m depth hard substrates were colonised by live solitary corals, including
 693 *Desmophyllum dianthus* and *Caryophyllia calveri*, with scattered to abundant frequencies and
 694 individuals measuring up to 5 cm in length. The upper portions and the flanks of the outcropping hard
 695 rock served as substrate for mainly fan-shaped, current-facing *Acanthogorgia hirsuta* colonies
 696 measuring up to 30 cm in length (Fig. 8H). Frequently, branches of soft corals and basal portions of
 697 solitary corals were also covered with red mud. The sponge *Tetrodictyum* cf. *tubulosum* was also
 698 observed in higher abundance in this red mud environment than in other parts of this canyon. The
 699 sponge *Farrea* sp. was also observed at this location but nowhere else in our study. Lower in the
 700 canyon (dive 407-11) a layer of fossil bivalves (*Neopycnodonte zibrowii*) was observed to play the
 701 role of a hard substrate for solitary corals. Further down, at the bottom of the canyon (725 m), we

702 found a thick layer of red mud so fluid that the ROV could not settle on the bottom to operate
 703 sampling tools (). No life could be seen on the muddy bottom.
 704



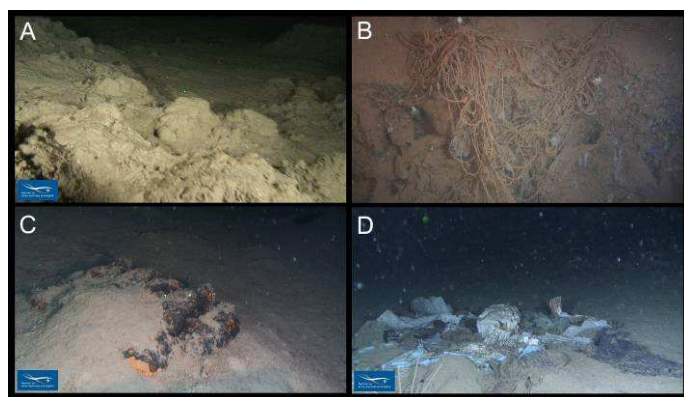
705
 706 **Fig. 12.** Distribution map of *Madrepora oculata* and red mud cover observed during dives in
 707 the Cassidaigne canyon.
 708

710 3.3.7 Distribution of anthropogenic litter

711 The highest abundance of litter was observed in the Toulon canyon in the Ligurian Sea (up to 12
 712 items.km⁻¹), while the highest abundance in the Gulf of Lion was observed in the Grand-Rhône canyon
 713 (up to 5 items.km⁻¹) (Fig. 2D). The canyons subject to less impact were the Sète and Marti canyons in
 714 which almost no debris was observed, except for plastics (100% in the Sète canyon) (Fig. 6F). The
 715 mean abundance was 3 items per km, 5 in the Ligurian Sea, and 1 in the Gulf of Lion.

716 The highest abundances of metals were found in the Toulon (9 items.km⁻¹) and Sicié
 717 (4 items.km⁻¹) canyons (Fig. 13C). Plastics were observed in every canyon, with the highest
 718 abundance occurring in the Planier canyon (2 items.km⁻¹) (Fig. 13D). Glass litter was observed
 719 eastwards from the Grand-Rhône (1 items.km⁻¹) to the Var canyons in the Ligurian Sea, with a peak in
 720 the Toulon (2 items.km⁻¹), La Ciotat (2 items.km⁻¹) and Sicié (2 items.km⁻¹) canyons. Wood debris
 721 was mainly located in the Stoechades canyon (0.4 items.km⁻¹) and on the Open slope (0.3 items.km⁻¹).
 722 Concrete, ceramics and other litter (fabrics and paper-board) were grouped together because they were
 723 not represented significantly.

724 Redundancy Analysis in the multiple linear regression procedure detected that the "Distance to
 725 the coast" variable accounted for 17% of the variance in the distribution of litter between canyons (p-
 726 value = 0.055). Mean depth, mean slope and navigation length did not provide a significant
 727 explanation of the distribution of litter between canyons.
 728



729
 730 **Fig. 13:** Anthropogenic impacts in canyons.
 731 **A:** Bathyal mud ploughed by trawling in the Montpellier canyon, MEDSEACAN cruise, dive P4,
 732 374 m. **B:** Fishing lines trapped on a rocky escarpment in the Cassidaigne canyon in an area

733 of bauxite red mud sedimentation, MARUM 2009, dive D7, 465 m. C: Metal litter (munitions)
734 in the Toulon canyon, MEDSEACAN cruise, dive P5, 495 m. D: Accumulation of soft plastic
735 litter in the Planier canyon, MEDSEACAN cruise, dive P8, 397 m.

736
737

738 4. Discussion

739

740 4.1 Distribution of benthic fishing resources and trawling impact

741

742 Fishing resources (marketable fishes, crustaceans and cephalopods) were statistically more
743 abundant in the Gulf of Lion than in the Ligurian Sea. This result further supports the well-known fact
744 that the Gulf of Lion is an area of high productivity compared to the other parts of the Mediterranean
745 Sea (Cartes et al., 2004). The amount of organic carbon enhancing the food chain results from the
746 arrival of cold and fresh water from the Rhône River, bringing organic and inorganic matter from
747 continental sources into the Gulf of Lion. The organic-matter-rich-sediment is intercepted by the heads
748 of shelf-incising canyons and transported down-slope where it provides food to benthic ecosystems
749 (Coll et al., 2010; Danovaro et al., 2010). Another factor that can explain the high concentration in
750 fishing resources in the Gulf of Lion is the consequence of its large continental shelf and exposure to a
751 cold and intense northern wind (Mistral), causing seasonal cooling and evaporation leading to the
752 formation and downwelling of dense surface sea-water.

753 The benthic fishes that were recognised in the video footage of this study are those that have
754 been frequently described on the upper slopes of the western Mediterranean Sea in previous studies in
755 which species were sampled by trawling, as in the "MEDiterranean International Bottom Trawl
756 Survey" (MEDITS) project (Bertrand, 2002; Cartes et al., 2002; D'Onghia et al., 2004; Demestre et al.,
757 2000; Morfin et al., 2012). Optical imagery is a reliable tool for evaluate fish diversity, although it is
758 not efficient for stock assessment because of difficulties in estimating spatial density and due to the
759 escape behaviour of mobile species.

760 *Nephrops norvegicus* is a commercially important crustacean in the Mediterranean Sea. It is a
761 sedentary marine decapod known for its burrowing behaviour and dependence on the muddy seabed
762 sediments of the slope (Mytilineou and Sarda, 1995; Sarda, 1998). Their higher abundance in the Gulf
763 of Lion is probably due to their preference for fine-grained sediment environments with weak
764 hydrodynamics (Maynou and Sarda, 1997; Tully and Hillis, 1995).

765 Several species of Octopodidae were observed in the video films though their identification was
766 not possible without sampling. The common octopus (*Octopus vulgaris*) and the horned octopus
767 (*Eledone cirrhosa*) are commercially important in the Mediterranean Sea and are caught by trawling
768 either on the continental shelf for juveniles or at greater depth for larger individuals (Sanchez et al.,
769 2004). Octopodidae were generally located in the Gulf of Lion. The highest abundance observed in the
770 Bourcart canyon is probably due to the rocky slab providing potential hiding and nesting places.
771 Species living on soft bottoms are probably different from those living in a rocky environment.

772 We assume that most of the specimens of Aristeidae encountered might be *Aristeus antennatus*,
773 which was often sampled during the MEDITS programme in the Gulf of Lion (Cau et al., 2002).
774 Aristeidae were located deeper and in lower abundance than other resources. These depths (< 500 m)
775 were explored by less than half of the MEDSEACAN dives, which could explain the low abundance
776 in Aristeidae observed in this study. Moreover Aristeidae have been observed previously down to
777 3000 m in the Balearic Islands (western Mediterranean Sea) (Cartes et al., 2009; Sarda et al., 2004).
778 The variability in the vertical distribution of *Aristeus antennatus* has been proved to be correlated to
779 the strong currents occurring during intense cascading events (DSWC) that displace individuals
780 towards greater depths over a ten-year time-scale (Company et al., 2008).

781 Other shrimp, such as the benthic-pelagic species *Plesionika* spp., were recorded in the video
782 films during the MEDSEACAN cruise. They were often located in high abundance in trawling scars
783 where no other benthic species could be seen. This is explained by the fact that these opportunistic
784 shrimp move into the trawling lane as a result of the temporary increase in food occurring due to the
785 increased mortality of organisms following the passage of trawls (Dimech et al., 2012; Ramsay et al.,
786 1998).

787 Trawling impacts were seen to occur in the same depth-range as marketable fishes, *Nephrops*
788 *norvegicus* and Octopodidae, which led us to assume that these species are targeted by bottom
789 trawling. Nevertheless, as Aristeidae are probably located deeper than the area explored, we could not
790 conclude on their "targeted species" status. In some other areas of the western Mediterranean Sea,
791 bottom trawling targeting the deep sea shrimp *Aristeus antennatus* is so intense that it has modified the
792 morphology of the sea floor above 800 m (Martín et al., 2013; Puig et al., 2012).

793

794 4.2 Distribution of Vulnerable Marine Ecosystem (VME) and anthropogenic impacts

795

796 Vulnerable Marine Ecosystems (VME) have been defined by OSPAR and the European
797 Commission as being any marine ecosystem whose integrity (i.e. ecosystem structure or function) is,
798 according to the best scientific information available and to the principle of precaution, threatened by
799 significant adverse impacts resulting from physical contact with bottom gears in the normal course of
800 fishing operations. Such ecosystems include, inter alia, reefs, seamounts, hydrothermal vents, cold-
801 water corals and cold-water sponge beds. The most vulnerable ecosystems are those that are easily
802 disturbed and whose recovery is either slow or impossible (European Commission, 2008). Bottom
803 trawling and long lines have been shown to have dramatic effects on the structure and functioning of
804 deep-sea ecosystems (Auster et al., 2011).

805

806 4.2.1 *Isidella elongata* communities and trawling impact on bathyal mud

807 We encountered few meadows of *I. elongata* in the Gulf of Lion (Bourcart, Marti and Petit-
808 Rhône), although these communities were frequently referenced in the past in the Mediterranean Sea
809 where they were described on the compact mud of the middle slope horizon between 500 and 1200 m
810 depth (Bellan-Santini et al., 2002; Cartes et al., 2004; Peres and Picard, 1964; Relini-Orsi and Relini,
811 1972).

812 Trawling scars were always seen at shallower depths than those of *I. elongata* colonies. We never
813 observed any overlap between the two vertical distributions. This led us to assume that *I. elongata* has
814 been swept away by repeated trawling in the shallowest part of its natural distribution. This gorgonian
815 species has practically disappeared from the Mediterranean Sea as it grows in areas targeted by
816 trawling (Cartes et al., 2009; Maynou and Cartes, 2012). Deep-water gorgonian corals are known to
817 grow slowly and live for hundreds of years (Risk et al., 2002; Williams et al., 2007), which implies a
818 long recovery time. Anthropogenic disturbance by trawling is thus devastating for these meadows of *I.*
819 *elongata*. They are considered as a sensitive habitat and efforts are being made to give them protected
820 status (GFCM, 2009a).

821 The highest density of *I. elongata* was located on a sloping seafloor (approx. 10 to 20°) in the
822 Petit-Rhône canyon. We assume that slopes provide protection from bottom trawling which cannot be
823 performed on sloping seafloors. Depth also provides protection from trawling, which is limited to
824 1000 m in the Mediterranean Sea (Sacchi, 2008). The sloping seafloor and deep seabed down to
825 1800 m on which *I. elongata* was observed during other cruises (M-C. Fabri, pers. obs.), may act as
826 refuge areas for this species. These refuge areas could be seen as locations where gorgonians could
827 reproduce and disseminate. Nevertheless, no study has been conducted to assess their potential
828 dispersion. Existing data on the growth rates of isidid octocorals are scarce but indicate slow annual
829 growth (Andrews et al., 2009). The life span of Isididae can reach 400 years (Sherwood et al., 2009).
830 Little is known about other important life history aspects of Isididae, such as reproduction, dispersal
831 and colonisation patterns.

832 Historical data suggest that *I. elongata*'s preferential habitat may be between gullies rather than in
833 canyons, a characteristic we observed three times during the MEDSEACAN cruise. Large meadows of
834 *I. elongata* were described in 1962 and 1964 between canyons (Carpine, 1964; Fredj, 1964; Maurin,
835 1962) (Fig.4). As the objective of the MEDSEACAN cruise did not focus on these areas, they should
836 be considered as an objective for a future cruise in order to check the actual condition of these
837 meadows and complete the present distribution of the species.

838

839 4.2.2 *Funiculina quadrangularis* communities and trawling impact on bathyal mud

840 We observed few *F. quadrangularis* in the video films. They were mainly located in the upper
841 part of the explored area. This Pennatulacea is known to characterise the upper slope horizon in the

842 soft muddy sediment between 180 and 400 m depth in the Mediterranean Sea (Bellan-Santini et al.,
843 2002; Cartes et al., 2004; Peres and Picard, 1964).

844 The inability of *F. quadrangularis* to withdraw into the sediment makes it sensitive to physical
845 disturbance (MacDonald et al., 1996). It is thought that this sea-pen has already disappeared from
846 many trawling locations. Indeed the commercial Norway lobster *Nephrops norvegicus* occupies the
847 same deep mud biotopes as Pennatulacea (Cartes et al., 2004). Trawls designed for *N. norvegicus*
848 scrape the seabed, removing emergent epifauna and leaving it flattened. The effect of trawling on the
849 sensitive *F. quadrangularis* makes it vulnerable. Although these Pennatulacea and their associated
850 habitats are not directly protected by legislation they are considered to be as "sensitive" habitats
851 worthy of conservation and more should be known about their distribution (GFCM, 2009a).

852 Trawling scars were always seen deeper than *F. quadrangularis* colonies. This led us to assume
853 that either *F. quadrangularis* has been swept away by repeated trawling in the deepest part of its
854 natural distribution, or it is located on the continental shelf as observed during the MEDITS cruise in
855 2012 (A. Jadaud, pers. comm.).

856 Historical data suggest that the preferential habitat of *F. quadrangularis* could be located between
857 gullies rather than in canyons. Large meadows of *F. quadrangularis* were described between canyons
858 in 1962 (Carpine, 1964; Fredj, 1964; Maurin, 1962) (Fig.4). As the objective of the MEDSEACAN
859 cruise did not focus on these areas, they should be considered as an objective for a future cruise in
860 order to check the actual condition of these meadows and complete the present distribution of the
861 species.

862

863 4.2.3 *Callogorgia verticillata* communities and lost fishing gears on rocky substrates

864 *Callogorgia verticillata* is an Alcyonacea that grows to a height of 1 m (Bo et al., 2012). It is a
865 suspension feeder forming large fans (1 m wide) oriented in the direction of the predominant current
866 and mainly observed on rocky outcrops (Sanchez et al., 2009). This species is often seen associated
867 with species of epifauna not observed in other communities, making this association unique
868 (Ophidiiformes *Benthocometes robustus*, Nudibranchia Tritoniidae, zoanthid *Isozoanthus primnoidus*).
869 The parasitic zoanthid *Isozoanthus primnoidus* (Carreiro-Silva et al., 2011) was observed on a single
870 colony in the Sicié canyon, whereas it has been observed more frequently in the Azores (Carreiro-
871 Silva et al., 2011). This zoanthid does not appear to be a threat for gorgonians.

872 The Bourcart canyon holds a particularly rich population of these colonies on a 900 meter long
873 cornice. This cornice was irregularly shaped as if covered by biogenic concretions, probably formed
874 when the level of the Mediterranean Sea was lower during the last glaciation period (Berné et al.,
875 1999; Lofi et al., 2003).

876 The high density of *C. verticillata* in the Bourcart canyon is unusual in the Mediterranean Sea
877 and has never been reported before. Many colonies of *C. verticillata* were entangled in bottom lines
878 and fishing nets. This led us to assume that the high diversity sheltered by the structure-forming
879 gorgonians is attractive for local fisheries even if the area is located far from the coast (60 km). In the
880 French canyons their recorded living depth, generally located around 350 m, is targeted by bottom line
881 fisheries.

882 From all these observations we propose that the fragile and poorly known *C. verticillata* should
883 be considered as a sensitive species deserving interest and protection. These *C. verticillata* colonies
884 have also been reported to be damaged by fishing activities on the continental shelf in the Tyrrhenian
885 Sea (Bo et al., 2012).

886

887 4.2.4 *Cold-water coral distribution*

888 The CWC populations in both the Lacaze-Duthiers and Cassidaigne canyons were visited
889 during the cruises described in this study. As previously known (Reyss, 1970; Zibrowius, 2003) the
890 two scleractinian species *Lophelia pertusa* and *Madrepora oculata* were present in the Lacaze-
891 Duthiers canyon (with *M. oculata* dominating over *L. pertusa*) while the single species *M. oculata* was
892 present in the Cassidaigne canyon.

893 In the Lacaze-Duthiers canyon, the largest colonies (> 50 cm) of *L. pertusa* were observed along
894 its western flank at two deep locations (350 m and 541 m depth), whereas colonies of *M. oculata* were
895 located on both flanks at shallower depths (246 to 531 m on the west flank; 260 m on the east flank).
896 The difference between the bathymetrical distribution pattern of *L. pertusa* and *M. oculata* could be

897 explained by the lower tolerance of *L. pertusa* to temperature variations, since it is known that they are
898 exposed to their maximal thermal limit in the Mediterranean Sea (Gori et al., 2013). To explain the
899 preferential distribution of the *L. pertusa* and *M. oculata* colonies on the west flank we can assume
900 that both flanks of the Lacaze-Duthiers canyon have different erosion regimes due to strong dense
901 shelf water cascading on this side of the Gulf of Lion, which is similar to what happens in the Cap de
902 Creus canyon (the next canyon westwards in Spanish waters). The bathymetric map (Fig. 7A) clearly
903 shows that the east flank of the canyon exhibits a smooth morphology whereas the west flank exhibits
904 steep slopes, probably due to an erosive regime (Orejas et al., 2009; Palanques et al., 2006). The
905 erosive regime results in three favourable conditions for CWC settlement: (1) a periodic nutritive
906 supply; (2) periodic washing of the sediment cover, leaving rocky outcrops available for settlement;
907 (3) a rapid drop in temperature at depth (Puig et al., 2008). Colonies were oriented horizontally or
908 downwards which is assumed to be a compromise between protection from the sediment flux and
909 exposure to water flow to ensure feeding (Gori et al., 2013).

910 The Cassidaigne canyon is the other location for dense populations of scleractinian corals and
911 sponges in the French Mediterranean Sea. The CWC community is exclusively located on the western
912 flank of the canyon. Due to the prevailing westerly shelf currents, the eastern flank of the Cassidaigne
913 canyon presents a prevalence of mud sediment draped over the bedrock, whereas the bedrock of the
914 opposing western flank is much more exposed and characterised by spurs, terraced rock ledges, karstic
915 dissolution features of former low sea-levels (e.g., the Messinian Salinity Crisis) and escarpments. The
916 broad canyon head is fed by three tributary gullies and two spurs on both the eastern and western
917 flanks form a bottleneck for the strong up- and downwelling hydrodynamic regime observed. On the
918 western spur high diversity was observed with a combination of species from the shelf and from the
919 CWC community. Mature *M. oculata* colonies grew mostly on the flanks of exposed bedrock. Small
920 colonies of *M. oculata* were observed covering vertical walls at two locations at 360 m and around
921 450 m depth. They were considered as on-going and active settlement events in the Cassidaigne
922 canyon.

923 We observed a high diversity of associated species in the Cassidaigne canyon. Deep
924 occurrences of *Corallium rubrum* colonies were recorded living together with *M. oculata* colonies on
925 the undersides of rock ledges or cave roofs from 200 to 325 m depth. This co-occurrence has been
926 described recently in the Sicilian Channel at 458 m depth off Malta and at 673 m in the Linosa Trough
927 (Costantini et al., 2010; Freiwald et al., 2009). Four species of Antipatharia (*Leiopathes glaberrima*,
928 *Parantipathes larix*, *Antipathella subpinnata* and *Antipathes* cf. *dichotoma*) were also present in high
929 abundance whereas they were not observed in the Lacaze-Duthiers canyon. This could be explained by
930 the heavy load of suspended particles observed in the Lacaze-Duthiers canyon associated with a strong
931 current that would be detrimental to the soft tissues of antipatharians (Wagner et al., 2012).

932 During the past decade, knowledge on live CWC communities in the Mediterranean Sea
933 supported by *L. pertusa*, *M. oculata* and to a lesser degree by *Dendrophyllia cornigera* has increased
934 considerably. Major coral hotspot areas are now known (Fink et al., 2013; Freiwald et al., 2009). The
935 two CWC locations described in this paper are different from each other. The Lacaze-Duthiers CWC
936 location is heavily loaded in particles and associated species are different from those in the
937 Cassidaigne canyon. The latter is one of the shallowest locations (210 m depth) together with the Strait
938 of Gibraltar (150 m depth, (Alvarez-Perez et al., 2005; De Mol et al., 2012) in which CWCs have been
939 found. The Lacaze-Duthiers canyon is geographically close and similar in composition to the CWC
940 community in the Cap de Creus canyon (Gori et al., 2013; Orejas et al., 2009).

941 The structure-forming CWC scleractinians of the Mediterranean Sea have been described to live
942 mostly on vertical walls (this study, (Freiwald et al., 2009). They have also been described on vertical
943 structures in the Atlantic canyons but to a greater extent, e.g., Whittard canyon, Bay of Biscay
944 (Huvenne et al., 2011). In the Mediterranean Sea, CWC communities are never as large as those found
945 in the Atlantic Ocean, where the prevailing conditions are more favourable with water temperatures
946 around 4°C and salinities around 35, whereas the Mediterranean Sea is a relatively warm (up to
947 13.8°C) and salty basin (salinity as high as 39). According to current knowledge of the temperature
948 limits for CWC, the Mediterranean Sea is close to the upper limit of many CWC occurring in the
949 bathyal zone (25.5°C for *M. oculata* in the Indian Ocean and 14.7°C for *L. pertusa* in the Atlantic
950 Ocean) (Keller and Os'kina, 2008).

951

952 4.2.4 Cold-water corals and lost fishing gears on rocky substrates

953 Lost fishing gears were observed in high densities together with CWC communities in both the
954 Lacaze-Duthiers and Cassidaigne canyons. This evidence of severe pressure from fishing shows that
955 these ecosystems therefore act as habitats for fishing resources as CWC communities are three
956 dimensional frameworks harbouring high diversity and a rich trophic network.

957 Long lines and ropes entangling colonies of CWC were evidence of this fishing pressure, but
958 these fishing gears represent only a percentage of the total effect of fishing on these CWC
959 communities as we assume that fishing equipment is not frequently lost. Nevertheless these three-
960 dimensional structures may be broken without any loss of equipment, as shown by the detached
961 colonies laying on the seafloor. Moreover scleractinians and associated species may be by-catch for
962 bottom long line fishing, therefore leaving no evidence (Sampaio et al., 2012).

963 In order to quantify the impact of fishing on hard substratum communities, account must be
964 taken not only of lost fishing gears but also of detached colonies. However, the detached colonies may
965 either be the result of the fishing pressure or due to their natural growth process. Indeed, the old basal
966 parts were infested by fixo-sessile communities (sponges, polychaetes, *Neopycnodonte cochlear*,
967 *Desmophyllum dianthus*) and excavated by bioeroding endobionts (Beuck et al., 2010), making them
968 fragile and heavier, finally causing them to fall. We can also add another impact caused by scientific
969 underwater vehicles which can encounter navigation difficulties in these complex environments,
970 resulting in breaking these luxuriant and fragile colonies.

971

972 4.2.5 Cold-water coral and bauxite red mud disposal

973 The Cassidaigne canyon is considerably affected by the massive disposal of bauxite residues
974 (Dauvin, 2010). These red residues are expelled by an aluminium company (operated successively by
975 Pechiney, Alcan, Rio Tinto, Alteo) located 40 km inland at Gardanne (Bouches-du-Rhône, France).
976 From 1967 to 1988, this red mud was discharged through two pipelines from two separate factories at
977 320 m depth near the canyon head. Since 1988, one of the factories stopped production and ceased
978 using one of the pipelines, resulting in the reduction of the discharge of red mud. For more than 45
979 years, this mud has spread along the canyon, on the lateral flanks and down to the abyssal plain,
980 contaminating the seabed with excess iron, titanium, vanadium and chromium (Fontanier et al., 2012).

981 Our visual inspection of the potential impact of the red mud on the benthic megafauna
982 underpins a selective negative if not potentially lethal effect, as the megafauna diversity observed in
983 2009 was lower than that observed in 1971 (Bourcier and Zibrowius, 1973). Moreover colonies of
984 gorgonians (*Acanthogorgia hirsuta*) were smothered with red mud and generally showed clear signs of
985 tissue necrosis and patches of mud flocs. Frequently, basal portions of cnidarians were covered by red
986 mud, although living parts were very clean, suggesting an effective mechanism against high
987 sedimentation rates.

988 The entire seabed along the canyon axis was covered by red mud below 350 m depth. The red
989 mud also draped steep inclined rock exposures and was found underneath overhangs. The episodically
990 severe up- and downwelling current regimes may be the driving force for the complete spatial
991 coverage of the natural seabed by man-made discharges. The burial of the rocky substrates suitable for
992 the settlement of *Madrepora oculata* prevent them from expanding deeper than 350 m. The few *M.*
993 *oculata* colonies observed deeper on blocks rising from the red mud bottom probably settled before
994 the start of the disposal of the red mud. The highest abundances of *M. oculata* in the red mud
995 environment were always observed on vertical walls where colonies were partly sheltered from silting.
996 These colonies seemed to cope with the heavy sedimentation load but at a metabolic cost that remains
997 to be investigated. However, it may point to a specific stress tolerance of *M. oculata*.

998 The recently settled colonies may be a positive result of the decrease in the red mud outflow
999 since 1988. The objective to stop the outflow by 2015 would certainly help these protected species to
1000 survive.

1001

1002 4.3 Distribution of anthropogenic litter

1003

1004 The economic impact of tourism, fishing and coastal urban populations has been demonstrated
1005 to be important in the north western Mediterranean sea, where different types of debris were found
1006 on the deep sea floor (Galvani et al., 1996). It was shown that only small amounts of debris were

1007 collected on the continental shelf from the Gulf of Lion whereas most of the debris was found in
1008 deeper areas, mainly in zones with high sedimentation rates such as submarine canyons. In our
1009 MEDSEACAN study, higher concentrations of litter were observed in the Ligurian Sea than in the
1010 Gulf of Lion. This is linked to the narrow continental shelf in this area, with more coastal canyons.
1011 This is also related to the general circulation of the water flowing to the south in the Gulf of Lion as a
1012 consequence of both strong Northwest winds and the very considerable discharge of the Rhone River.
1013 The highest concentrations of metal objects observed in both the Toulon and Sicié canyons were
1014 explained by the presence of a large military harbour with discarded equipment on the adjacent sea
1015 floor, including weapons and ammunition. Plastics were found everywhere, with a percentage to total
1016 debris up to 100 in the Sète canyon, but in low abundance, within the same range as that described
1017 previously (Barnes et al., 2009; Galgani et al., 2000; Mordecai et al., 2011; Ramirez-Llodra et al.,
1018 2011). Pieces of glass, mainly beer bottles, were observed in the Ligurian Sea and linked to both
1019 pleasure boats and cruising ships. The Stoechades canyon contained quantities of wood debris coming
1020 from adjacent woods and forests from the three islands of Port-Cros, Porquerolles and Levant.
1021 Fishing-related objects were found in coastal canyons only, as a consequence of fishing activity.
1022 Finally, ceramics and other litter were spread everywhere but only in small quantities.

1023 As mentioned previously (Galgani et al., 1996) debris in rocky environments cannot be
1024 evaluated by trawling. Video recording is therefore a valuable approach for evaluating litter which is
1025 often trapped in the rocky areas such as slopes. The mean concentration of litter calculated from
1026 submersible (Cyana) dives at the bottom of canyons were 24 items.km⁻¹ (Galgani et al., 1996) on
1027 average, while the mean concentration measured on slopes in this study was 3 items.km⁻¹, which is far
1028 less. From both studies, it is clear that the amount of litter should not be considered as decreasing with
1029 time. We link this typical situation to several causes: (1) we explored the flanks of the canyons during
1030 the MEDSEACAN cruise on which the litter does not tend to accumulate; (2) the intensity of the light
1031 and the small area covered by the camera used with a small ROV such as Super Achille are
1032 respectively lower and narrower (1 meter in width) than with the manned submersible Cyana. The
1033 latter enabled surveying a strip 4-5 meters wide on soft bottoms. Overall, the analysis of results
1034 provides more detailed information on the diversity of debris typically related to coastal activities
1035 including fishing, harbours and tourism.

1036

1037 4.4 *Vulnerable Marine Ecosystems and their preservation*

1038

1039 Different international organisations (International Council for the Exploration of the Sea ICES,
1040 United Nations, European Commission, General Fisheries Commission for the Mediterranean GFCM)
1041 and Conventions (OSPAR, CITES and Barcelona convention) have recommended protection and
1042 management of a list of species and habitats that are either "sensitive", "vulnerable", "threatened" or
1043 "in decline", among which some are found in deep-sea ecosystems. All these conventions have led to
1044 the establishment of Marine Protected Areas (MPA) in all the world's oceans. Three MPAs and one
1045 fishing area with restricted access have been created recently in the French part of the Mediterranean
1046 Sea (Fig. 14).

1047 The "Parc Marin du Golfe du Lion" (decree 2011-1269) includes CWC communities of the
1048 Lacaze-Duthiers canyon and *Isidella elongata* communities of the Bourcart canyon. This park should
1049 implement new regulations to protect these areas against bottom fishing which is the most direct and
1050 the most noticeable threat to these ecosystems. Another specific site to be protected in this park is the
1051 rocky slab in the Bourcart canyon with high diversity associated with *Callogorgia verticillata*
1052 colonies.

1053 The "Parc National des Calanques" (decree 2012-507) including the CWC communities of
1054 Cassidaigne canyon has defined several areas with specific regulations. Two of them are delimited on
1055 the western flank of Cassidaigne canyon: a "reinforced protection zone" and a "no-take zone". The
1056 "reinforced protection zone" is a "no-take zone" with some exceptions for local artisanal fishermen
1057 who were making their living there before the creation of the park. These two special zones have been
1058 defined to protect CWC communities from fishing. The "reinforced protection zone" allowing
1059 exceptional fishing is not located at the CWC location but at that where the disposal of red mud
1060 occurs. CWC communities are protected from fishing (long lines and nets) but not from the red mud
1061 discharged in this canyon which will cause long term disturbance even after the end of disposal.

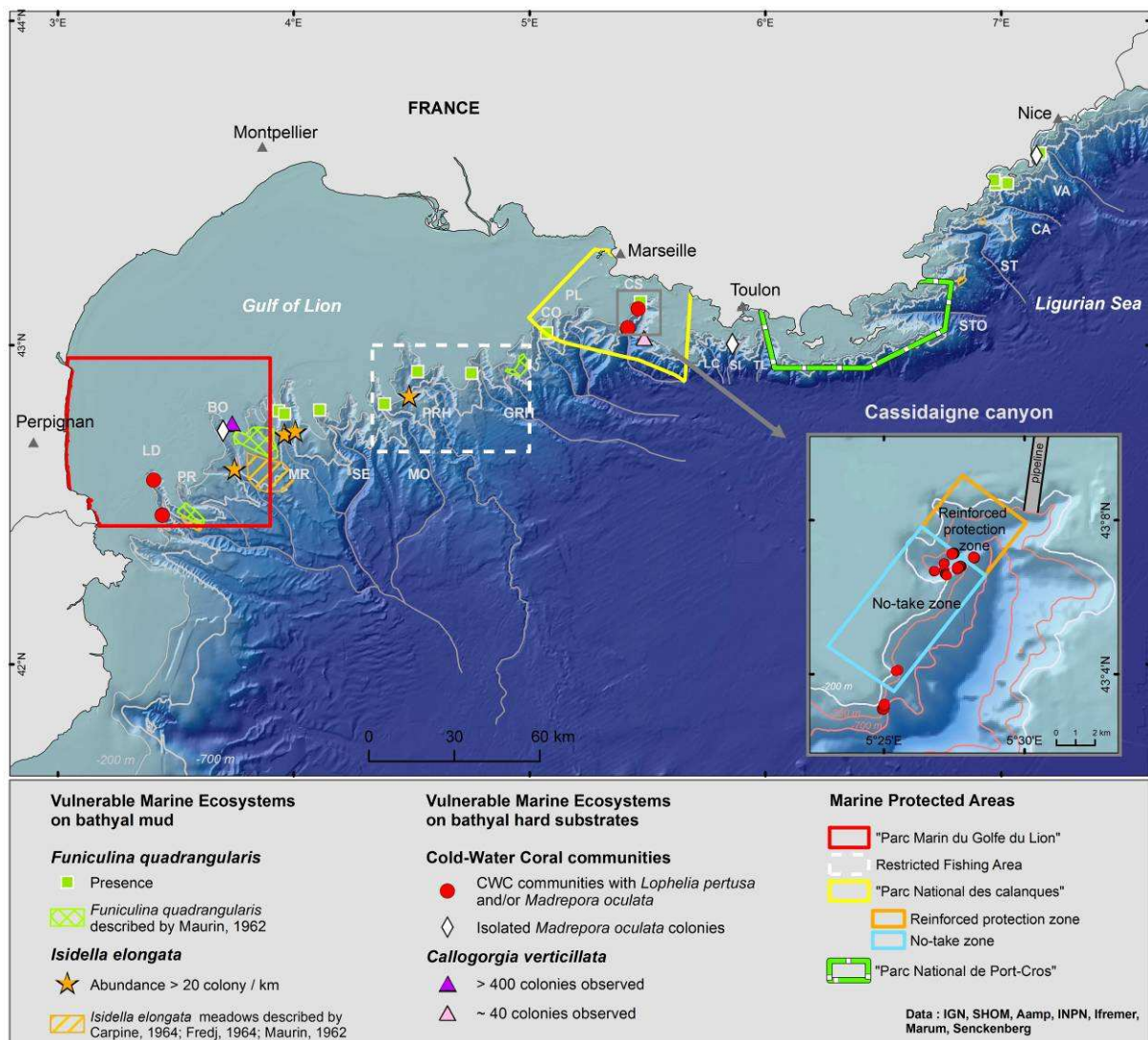
1062 Contamination of the trophic chain could occur in the future when red mud disposal will stop in 2015,
 1063 causing a change in environmental conditions and possibly leading to the release of heavy metals into
 1064 the environment (Fontanier et al., 2012). Contamination of the trophic chain in the Cassidaigne canyon
 1065 by heavy metals could lead to sanitary consequences. Based on the precautionary principle we think
 1066 fishing should be completely prohibited in Cassidaigne canyon. New studies will be launched to study
 1067 this potential contamination by heavy metals.

1068 The "Parc National de Port-Cros" (decree 2012-649) has been recently extended to include the
 1069 adjacent bathyal seafloor, where we referenced no vulnerable ecosystems.

1070 Additionally, the Scientific Advisory Committee of the GFCM has set up a fishing area with
 1071 restricted access off the French coast in the Gulf of Lion, in which the fishing effort shall not exceed
 1072 the level of fishing effort applied in 2008 (GFCM, 2009b). This area includes the Montpellier, Petit-
 1073 Rhône and Grand-Rhône canyons and has been designated as a refuge from trawling for a non-
 1074 exploited spawning fraction of the demersal fishing stock (Farrugio, 2012). However, this area has not
 1075 been designated for the protection of sensitive ecosystems, despite the fact that the fishing effort has
 1076 been limited to present levels since 2008. Nonetheless the benthic ecosystems may have been
 1077 damaged already.

1078 Vessel Monitoring System (VMS) data could be used in order to highlight areas of heavy
 1079 fishing pressure. Afterwards, the data collected from these areas should be crossed with VME spatial
 1080 distribution data to set up specific conservative measures.

1081
 1082



1083

1084 **Fig. 14.** Geographical localisation of the Vulnerable Marine Ecosystems and the Marine
1085 Protected Areas of the French continental coast of the Mediterranean Sea. Submarine
1086 canyons from West to East: LD: Lacaze-Duthiers, PR: Pruvost, BO: Bourcart (Aude), MR: Marti
1087 (Hérault), SE: Sète, MO: Montpellier, PRH: Petit Rhône, GRH: Grand Rhône, CO: Couronne, PL:
1088 Planier, CS: Cassidaigne, LC: La Ciotat, SI: Sicié, TL: Toulon, STO: Stoechades, ST: Saint-Tropez
1089 (not considered in this study), CA: Cannes, VA: Var.

1090
1091
1092
1093
1094
1095
1096
1097
1098
1099
1100
1101

1102 **5. Conclusions**

1103
1104
1105
1106
1107
1108

Video data were used to carry out an inventory of the distributions of benthic communities in the heads of French canyons considered to be vulnerable to anthropogenic impacts. This study is the first to have enabled: (1) the comparison of 17 canyons sampled in the same bathymetrical range over a limited temporal timescale (1 year), and (2) the observation of the soft substrate of Vulnerable Marine Ecosystems (VME) in situ instead of sampling by trawling or coring.

1109 The Canyons of the Gulf of Lion are different from those of the Ligurian Sea with regard to
1110 their abundance in resources, VME fauna, substrates and anthropogenic impacts. Soft bottom VME
1111 fauna (*Isidella elongata* and *Funiculina quadrangularis*), resources and trawling impacts were mainly
1112 located in the Gulf of Lion. These VME fauna seem to have been swept away by repeated trawling.
1113 Access to Vessel Monitoring System data could help to better evaluate fishing impacts on these
1114 communities.

1115 Cold-water coral communities (*Lophelia pertusa*, *Madrepora oculata*) are present in two of the
1116 French canyons (Lacaze-Duthiers and Cassidaigne). Fishing and silting (e.g. red mud) are the major
1117 impacts affecting these ecosystems presenting high diversity. We propose that the community of the
1118 gorgonian *Callogorgia verticillata* should be considered a VME taxa as it was rarely observed, it has
1119 been severely impacted and is associated with a high species diversity.

1120 All these VME fauna are located in the recently created Marine Protected Areas where new
1121 regulations including deep-sea ecosystem conservative measures must be drafted.

1122 This initial assessment of VME distribution was performed using historical and recent available
1123 data. New data must be collected for the future assessment of the ecological status of benthic
1124 ecosystems to be carried out as part of the Marine Strategy Framework Directive.

1125

1126 **Acknowledgments**

1127 We are grateful to the Agency for Marine Protected Areas (Aamp) and especially to Pierre Watremez
1128 for coordinating and organising the MEDSEACAN cruise, providing the video films and reading the
1129 manuscript. We also thank all the participants of the MEDSEACAN, MARUM 2009, MARUM-
1130 Senckenberg 2011, ESSROV 2010, CYATOX 1995 cruises. The authors thank the captain, and the
1131 crew of the R/V "Minibex" and the Comex team for their professionalism in operating the ROV Super
1132 Achille and Submersible Remora. Thanks are also extended to O. Soubigou, G. Clodic, B. Loubrieu
1133 from Ifremer for their help, respectively, with the "Adelie" software, video film formatting and the
1134 bathymetric surveys of the Mediterranean Sea. Furthermore we are indebted to Keith Hodson
1135 (www.accent-europe.fr) for correcting the English. The authors also thank the reviewers for their
1136 helpful comments to improve the manuscript.

1137 *This paper was written in the framework of the Marine Strategy Directive (MSFD), with the support of*
1138 *the French Ministry of Ecology, Sustainable Development and Energy (convention 11/1219231/NF).*
1139 *LB, DH and AF received support from the EU-FP VII projects HERMIONE (contract number 226354)*
1140 *and LB and AF from CoralFISH (contract number 213144).*

1141
1142
1143

1144 **References**

1145

1146 Alberola, C., Millot, C., 2003. Circulation in the French Mediterranean coastal zone near Marseilles:
1147 the influence of wind and the Northern Current. *Continental Shelf Research* 23, 587-
1148 610.10.1016/s0278-4343(03)00002-5

1149 Alvarez-Perez, G., Busquets, P., De Mol, B., Sandoval, N.G., Canals, M., Casamor, J.L., 2005. Deep-
1150 water coral occurrences in the Strait of Gibraltar, in: Freiwald, A., Roberts, J.M. (Eds.), *Cold-
1151 Water Corals and Ecosystems*. Springer, pp. 207-221.

1152 Andrews, A.H., Stone, R.P., Lundstrom, C.C., DeVogelaere, A.P., 2009. Growth rate and age
1153 determination of bamboo corals from the northeastern Pacific Ocean using refined ²¹⁰Pb
1154 dating. *Mar. Ecol. Prog. Ser.* 397, 173-185

1155 Astraldi, M., Balopoulos, S., Candela, J., Font, J., Gacic, M., Gasparini, G.P., Manca, B., Theocharis,
1156 A., Tintore, J., 1999. The role of straits and channels in understanding the characteristics of
1157 Mediterranean circulation. *Progress in Oceanography* 44, 65-108.10.1016/s0079-
1158 6611(99)00021-x

1159 Auster, P.J., Gjerde, K., Heupel, E., Watling, L., Grehan, A., Rogers, A.D., 2011. Definition and
1160 detection of vulnerable marine ecosystems on the high seas: problems with the “move-on”
1161 rule. *ICES Journal of Marine Science: Journal du Conseil* 68, 254-264.10.1093/icesjms/fsq074

1162 Barnes, D.K.A., Galgani, F., Thompson, R.C., Barlaz, M., 2009. Accumulation and fragmentation of
1163 plastic debris in global environments. *Philosophical Transactions of the Royal Society B-
1164 Biological Sciences* 364, 1985-1998.10.1098/rstb.2008.0205

1165 Bellan-Santini, D., Bellan, G., Bittar, G., Harmelin, J.G., Pergent, G., 2002. Handbook for interpreting
1166 types of marine habitat for the selection of sites to be included in the national inventories of
1167 natural sites of conservation interest, UNEP Report, Tunis, p. 217.

1168 Berné, S., 2000. Campagne Marion - Zone Bourcart, Golfe du Lion (10m). Ifremer, Plouzané.

1169 Berné, S., Loubrieu, B., equipe Calmar, 1999. Canyons and recent sedimentary processes on the
1170 western Gulf of Lions margin. First results of the Calmar cruise. *Comptes Rendus De
1171 l'Academie des sciences Serie II Fascicule a-Sciences de la Terre et des Planètes* 328, 471-477

1172 Bertrand, J.A., 2002. Mediterranean marine demersal resources: The medits international trawl survey
1173 (1994-1999) - Foreword. *Scientia Marina* 66, 5-7

1174 Beuck, L., Freiwald, A., Taviani, M., 2010. Spatiotemporal bioerosion patterns in deep-water
1175 scleractinians from off Santa Maria di Leuca (Apulia, Ionian Sea). *Deep-Sea Research II* 57,
1176 458-470.10.1016/j.dsr2.2009.08.019

1177 Bo, M., Canese, S., Spaggiari, C., Pusceddu, A., Bertolino, M., Angiolillo, M., Giusti, M., Loreto,
1178 M.F., Salvati, E., Greco, S., Bavestrello, G., 2012. Deep coral oases in the South Tyrrhenian
1179 Sea. *Plos One* 7, e49870.10.1371/journal.pone.0049870

1180 Bouchet, P., 2006. The magnitude of marine biodiversity, in: Duarte, C.M. (Ed.), *The Exploration of
1181 Marine Biodiversity*, pp. 32-64.

1182 Bourcier, M., Zibrowius, H., 1973. Les "boues rouges" déversées dans le canyon de la Cassidaigne :
1183 Observations en soucoupe plongeante SP350 (Juin 1971) et résultats de dragages. *Tethys* 4,
1184 811-842

1185 Canals, M., Puig, P., Durrieu de Madron, X., Heussner, S., Palanques, A., Fabres, J., 2006. Flushing
1186 submarine canyons. *Nature* 444, 354-357.10.1038/nature05271

1187 Carpine, C., 1964. La côte de l'Esterel, de la pointe des Lions à la pointe de l'Aiguille (Région A2) -
1188 Fascicule 3. *Bull. Inst. océanogr. Monaco* 63, 1-52

1189 Carreiro-Silva, M., Braga-Henriques, A., Sampaio, I., de Matos, V., Porteiro, F.M., Ocana, O., 2011.
1190 *Isozoanthus primnoidus*, a new species of zoanthid (Cnidaria: Zoantharia) associated with the

- 1191 gorgonian *Callogorgia verticillata* (Cnidaria: Alcyonacea). *Ices Journal of Marine Science* 68,
1192 408-415.10.1093/icesjms/fsq073
- 1193 Cartes, J.E., Abello, P., Lloris, D., Carbonell, A., Torres, P., Maynou, F., De Sola, L.G., 2002. Feeding
1194 guilds of western Mediterranean demersal fish and crustaceans: an analysis based on a spring
1195 survey. *Scientia Marina* 66, 209-220
- 1196 Cartes, J.E., Maynou, F., Lloris Samo, D., Gil Sola, L., García, M., 2009. Influence of trawl type on
1197 the composition and diversity of deep benthopelagic fish and decapod assemblages off the
1198 Catalan coasts (western Mediterranean). *Scientia Marina* 73, 725-737
- 1199 Cartes, J.E., Maynou, F., Sardà, F., Company, J.B., Lloris Samo, D., Turdela, S., 2004. The
1200 Mediterranean deep-sea ecosystems Part I: An overview of their diversity, structure,
1201 functioning and anthropogenic impacts. 9-38.
- 1202 Cau, A., Carbonell, A., Follesa, M.C., Mannini, A., Norrito, G., Orsi-Relini, L., Politou, C.Y.,
1203 Ragonese, S., Rinelli, P., 2002. MEDITS-based information on the deep-water red shrimps
1204 *Aristaeomorpha foliacea* and *Aristeus antennatus* (Crustacea : Decapoda : Aristeidae).
1205 *Scientia Marina* 66, 103-124
- 1206 Clarke, K.R., Warwick, R.M., 2001. Change in marine communities: an approach to statistical analysis
1207 and interpretation, 2nd edition.
- 1208 Coll, M., Piroddi, C., Steenbeek, J., Kaschner, K., Ben Rais Lasram, F., Aguzzi, J., Ballesteros, E.,
1209 Bianchi, C.N., Corbera, J., Dailianis, T., Danovaro, R., Estrada, M., Froggia, C., Galil, B.S.,
1210 Gasol, J.M., Gertwagen, R., Gil, J., Guilhaumon, F., Kesner-Reyes, K., Kitsos, M.-S.,
1211 Koukouras, A., Lampadariou, N., Laxamana, E., Lopez-Fe de la Cuadra, C.M., Lotze, H.K.,
1212 Martin, D., Mouillot, D., Oro, D., Raicevich, S., Rius-Barile, J., Saiz-Salinas, J.I., San
1213 Vicente, C., Somot, S., Templado, J., Turon, X., Vafidis, D., Villanueva, R., Voultsiadou, E.,
1214 2010. The biodiversity of the Mediterranean Sea: estimates, patterns, and threats. *Plos One* 5,
1215 e11842
- 1216 Company, J.B., Puig, P., Sarda, F., Palanques, A., Latasa, M., Scharek, R., 2008. Climate Influence on
1217 deep sea populations. *Plos One* 3, e1431.10.1371/journal.pone.0001431
- 1218 Costantini, F., Taviani, M., Remia, A., Pintus, E., Schembri, P.J., Abbiati, M., 2010. Deep-water
1219 *Corallium rubrum* (L., 1758) from the Mediterranean Sea: preliminary genetic
1220 characterisation. *Marine Ecology-an Evolutionary Perspective* 31, 261-269.10.1111/j.1439-
1221 0485.2009.00333.x
- 1222 Costello, M.J., Coll, M., Danovaro, R., Halpin, P., Ojaveer, H., Miloslavich, P., 2010. A census of
1223 marine biodiversity knowledge, resources, and future challenges. *Plos One* 5, e12110
- 1224 D'Onghia, G., Politou, C.Y., Bozzano, A., Lloris, D., Rotllant, G., Sion, L., Mastrototaro, F., 2004.
1225 Deep-water fish assemblages in the Mediterranean Sea. *Scientia Marina* 68, 87-99
- 1226 Danovaro, R., Company, J.B., Corinaldesi, C., D'Onghia, G., Galil, B.S., Gambi, C., Gooday, A.,
1227 Lampadariou, N., Luna, G.M., Morigi, C., Olu, K., Polymenakou, P., Ramirez-Llodra, E.,
1228 Sabbatini, A., Sarda, F., Sibuet, M., Tselepides, A., 2010. Deep-sea biodiversity in the
1229 Mediterranean Sea: The known, the unknown, and the knowable. *Plos One* 5, e11832
- 1230 Dauvin, J.C., 2010. Towards an impact assessment of bauxite red mud waste on the knowledge of the
1231 structure and functions of bathyal ecosystems: The example of the Cassidaigne canyon (north-
1232 western Mediterranean Sea). *Marine Pollution Bulletin* 60, 197-
1233 206.10.1016/j.marpolbul.2009.09.026
- 1234 De Mol, B., Amblas, D., Alvarez, G., Busquets, P., Calafat, A., Canals, M., Duran, R., Lavoie, C.,
1235 Acosta, J., Munoz, A., 2012. Cold-water coral distribution in an erosional environment: the
1236 Strait of Gibraltar, in: Harris, P.T., Baker, E.K. (Eds.), *Seafloor Geomorphology as Benthic
1237 Habitat*. Elsevier, Amsterdam, pp. 635-643.
- 1238 Demestre, M., Sanchez, P., Abello, P., 2000. Demersal fish assemblages and habitat characteristics on
1239 the continental shelf and upper slope of the north-western Mediterranean. *Journal of the
1240 Marine Biological Association of the United Kingdom* 80, 981-
1241 988.10.1017/s0025315400003040
- 1242 Dimech, M., Kaiser, M.J., Ragonese, S., Schembri, P.J., 2012. Ecosystem effects of fishing on the
1243 continental slope in the Central Mediterranean Sea. *Marine Ecology-Progress Series* 449, 41-
1244 54.10.3354/meps09475

- 1245 Durrieu de Madron, X., Zervakis, V., Theocharis, A., Georgopoulos, D., 2005. Comments on
 1246 "Cascades of dense water around the world ocean". *Progress in Oceanography* 64, 83-
 1247 90.10.1016/j.pocean.2004.08.004
- 1248 European Commission, 2008. Regulation (EC 734/2008) on the protection of vulnerable marine
 1249 ecosystems in the high seas from the adverse impacts of bottom fishing gears. Official Journal
 1250 of the European Union
- 1251 FAO, 2009. Report of the technical consultation on international guidelines for the management of
 1252 deep-sea fisheries in the high seas. 881, FAO, 98.
- 1253 Farrugio, H., 2012. A refugium for the spawners of exploited Mediterranean marine species: the
 1254 canyons of the continental slope of the Gulf of Lion, in: Wurtz, M. (Ed.), *Mediterranean
 1255 Submarine Canyons : Ecology and Governance*. IUCN, Gland, Switzerland and Malaga,
 1256 Spain, pp. 45-49.
- 1257 Fink, H.G., Wienberg, C., De Pol-Holz, R., Wintersteller, P., Hebbeln, D., 2013. Cold-water coral
 1258 growth in the Alboran Sea related to high productivity during the Late Pleistocene and
 1259 Holocene. *Marine Geology* 339, 71-82
- 1260 Fontanier, C., Fabri, M.C., Buscail, R., Biscara, L., Koho, K., Reichart, G.J., Cossa, D., Galaup, S.,
 1261 Chabaud, G., Pigot, L., 2012. Deep-sea foraminifera from the Cassidaigne Canyon (NW
 1262 Mediterranean): Assessing the environmental impact of bauxite red mud disposal. *Marine
 1263 Pollution Bulletin* 64, 1895-1910.10.1016/j.marpolbul.2012.06.016
- 1264 Fredj, G., 1964. La région de Saint-Tropez: du cap Taillat au cap de Saint-Tropez (Région A1) -
 1265 Fascicule 2. *Bull. Inst. océanogr. Monaco* 63, 1-55
- 1266 Freiwald, A., Beuck, L., Rüggeberg, A., Taviani, M., Hebbeln, D., 2009. The white coral community
 1267 in the Central Mediterranean Sea revealed by ROV Surveys. *Oceanography* 22, 58-74
- 1268 Galgani, F., Leaute, J.P., Moguedet, P., Souplet, A., Verin, Y., Carpentier, A., Goraguer, H., Latrouite,
 1269 D., Andral, B., Cadiou, Y., Mahe, J.C., Poulard, J.C., Nerisson, P., 2000. Litter on the sea
 1270 floor along European coasts. *Marine Pollution Bulletin* 40, 516-527
- 1271 Galgani, F., Souplet, A., Cadiou, Y., 1996. Accumulation of debris on the deep sea floor off the
 1272 French Mediterranean coast. *Marine Ecology-Progress Series* 142, 225-234
- 1273 GFCM, S.A.C., 2009a. Criteria for the identification of sensitive habitats of relevance for the
 1274 management of priority species (General Fisheries Commission for the Mediterranean). 3.
- 1275 GFCM, S.A.C., 2009b. On the establishment of a Fisheries Restricted Area in the Gulf of Lions to
 1276 protect spawning aggregations and deep sea sensitive habitats (GFCM/33/2009/1).
- 1277 Gori, A., Orejas, C., Madurell, T., Bramanti, L., Martins, M., Quintanilla, E., Marti-Puig, P., Lo
 1278 Iacono, C., Puig, P., Requena, S., Greenacre, M., Gili, J.M., 2013. Bathymetrical distribution
 1279 and size structure of cold-water coral populations in the Cap de Creus and Lacaze-Duthiers
 1280 canyons (northwestern Mediterranean). *Biogeosciences* 10, 2049-2060.10.5194/bg-10-2049-
 1281 2013
- 1282 Greene, H.G., Bizzarro, J.J., 2007. Construction of digital potential marine benthic habitat maps using
 1283 a code classification scheme and its application, in: Todd, B.J., Greene, H.G. (Eds.), *Mapping
 1284 the Seafloor for Habitat Characterization: Geological Association of Canada*, pp. 145-159.
- 1285 Harris, P.T., Whiteway, T., 2011. Global distribution of large submarine canyons: Geomorphic
 1286 differences between active and passive continental margins. *Marine Geology* 285, 69-
 1287 86.10.1016/j.margeo.2011.05.008
- 1288 Huvenne, V.A.I., Tyler, P.A., Masson, D.G., Fisher, E.H., Hauton, C., Huehnerbach, V., Le Bas, T.P.,
 1289 Wolff, G.A., 2011. A Picture on the wall: Innovative mapping reveals cold-water coral refuge
 1290 in submarine canyon. *Plos One* 6, e28755.e28755
 1291 10.1371/journal.pone.0028755
- 1292 Keller, N.B., Os'kina, N.S., 2008. Habitat temperature ranges of azooxantellate scleractinian corals in
 1293 the World Ocean. *Oceanology* 48, 77-84.10.1134/s0001437008010098
- 1294 Lofi, J., Rabineau, M., Gorini, C., Berne, S., Clauzon, G., De Clarens, P., Dos Reis, A.T., Mountain,
 1295 G.S., Ryan, W.B.F., Steckler, M.S., Fouchet, C., 2003. Plio-Quaternary prograding clinoform
 1296 wedges of the western Gulf of Lion continental margin (NW Mediterranean) after the
 1297 Messinian Salinity Crisis. *Marine Geology* 198, 289-317.10.1016/s0025-3227(03)00120-8
- 1298 Loubrieu, B., Satra, C., 2010. Bathy-morphologie du plateau continental - Façades Méditerranéenne et
 1299 Corse (édition 2010, 100 m). Ifremer, Plouzané, p. Modèle bathymétrique (MNT) à 100m de

1300 résolution de la façade maritime française de la Méditerranée. Le MNT a été réalisé par
1301 krigeage à partir d'une compilation des principales sources de données bathymétriques
1302 françaises.

1303 MacDonald, D.S., Little, M., Eno, N.C., Hiscock, K., 1996. Disturbance of benthic species by fishing
1304 activities: A sensitivity index. *Aquatic Conservation-Marine and Freshwater Ecosystems* 6,
1305 257-268.10.1002/(sici)1099-0755(199612)6:4<257::aid-aqc194>3.3.co;2-z

1306 Martín, J., Puig, P., Palanques, A., Ribó, M., 2013. Trawling-induced daily sediment resuspension in
1307 the flank of a Mediterranean submarine canyon. *Deep Sea Research II* (this
1308 issue).<http://dx.doi.org/10.1016/j.dsr2.2013.05.036>

1309 Maurin, C., 1962. Étude des fonds chalutables de la Méditerranée occidentale (Écologie et Pêche).
1310 *Rev. Trav. Inst. Pêche marit.* 26, 163-220

1311 Maynou, F., Cartes, J.E., 2012. Effects of trawling on fish and invertebrates from deep-sea coral fades
1312 of *Isidella elongata* in the western Mediterranean. *Journal of the Marine Biological*
1313 *Association of the United Kingdom* 92, 1501-1507.10.1017/s0025315411001603

1314 Maynou, F., Sarda, F., 1997. *Nephrops norvegicus* population and morphometrical characteristics in
1315 relation to substrate heterogeneity. *Fisheries Research* 30, 139-149.10.1016/s0165-
1316 7836(96)00549-8

1317 Millot, C., 1990. The Gulf of Lions' hydrodynamics. *Continental Shelf Research* 10, 885-894

1318 Mordecai, G., Tyler, P.A., Masson, D.G., Huvenne, V.A.I., 2011. Litter in submarine canyons off the
1319 west coast of Portugal. *Deep-Sea Research II* 58, 2489-2496.10.1016/j.dsr2.2011.08.009

1320 Morfin, M., Fromentin, J.-M., Jadaud, A., Bez, N., 2012. Spatio-temporal patterns of key exploited
1321 marine species in the Northwestern Mediterranean Sea. *Plos One* 7, e37907.e37907
1322 10.1371/journal.pone.0037907

1323 Mytilineou, C., Sarda, F., 1995. Age and growth of *Nephrops norvegicus* in the Catalan Sea, using
1324 length-frequency analysis. *Fisheries Research* 23, 283-299.10.1016/0165-7836(94)00350-6

1325 Orejas, C., Gori, A., Lo Iacono, C., Puig, P., Gili, J.M., Dale, M.R.T., 2009. Cold-water corals in the
1326 Cap de Creus canyon, northwestern Mediterranean: spatial distribution, density and
1327 anthropogenic impact. *Marine Ecology-Progress Series* 397, 37-51.10.3354/mep08314

1328 Palanques, A., Durrieu de Madron, X., Puig, P., Fabres, J., Guillen, J., Calafat, A., Canals, M.,
1329 Heussner, S., Bonnin, J., 2006. Suspended sediment fluxes and transport processes in the Gulf
1330 of Lions submarine canyons. The role of storms and dense water cascading. *Marine Geology*
1331 234, 43-61.10.1016/j.margeo.2006.09.002

1332 Peres, J.M., Picard, J., 1964. Nouveau Manuel de Bionomie benthique de la mer Méditerranée.
1333 *Recueil des travaux de la Station Marine d'Endoume* 31, 1-137

1334 Puig, P., Canals, M., Company, J.B., Martin, J., Amblas, D., Lastras, G., Palanques, A., Calafat, A.M.,
1335 2012. Ploughing the deep sea floor. *Nature* 489, 286-289.10.1038/nature11410

1336 Puig, P., Palanques, A., Orange, D.L., Lastras, G., Canals, M., 2008. Dense shelf water cascades and
1337 sedimentary furrow formation in the Cap de Creus Canyon, northwestern Mediterranean Sea.
1338 *Continental Shelf Research* 28, 2017-2030.10.1016/j.csr.2008.05.002

1339 Ramirez-Llodra, E., Tyler, P.A., Baker, M.C., Bergstad, O.A., Clark, M.R., Escobar, E., Levin, L.A.,
1340 Menot, L., Rowden, A.A., Smith, C.R., Van Dover, C.L., 2011. Man and the last great
1341 wilderness: human impact on the deep sea. *Plos One* 6, e22588

1342 Ramsay, K., Kaiser, M.J., Hughes, R.N., 1998. Responses of benthic scavengers to fishing disturbance
1343 by towed gears in different habitats. *Journal of Experimental Marine Biology and Ecology*
1344 224, 73-89.10.1016/s0022-0981(97)00170-6

1345 Relini-Orsi, L., Relini, G., 1972. Note sui Crostacei Decapodi batiali del Mar Ligure. *Boll. Mus. Ist*
1346 *Biol. Univ. Genova* 40, 47-73

1347 Reyss, D., 1970. Bionomie benthique de deux canyons sous-marins de la mer Catalane: le Rech du
1348 Cap et le Rech Lacaze-Duthiers, Paris. Université de Paris VI, p. 255.

1349 Risk, M.J., Heikoop, J.M., Snow, M.G., Beukens, R., 2002. Lifespans and growth patterns of two
1350 deep-sea corals: *Primnoa resedaeformis* and *Desmophyllum cristagalli*. *Hydrobiologia* 471,
1351 125-131

1352 Sacchi, J., 2008. The use of trawling nets in the Mediterranean. Problems and selectivity options.
1353 *Options Méditerranéennes Series B*, 87-96

1354 Sampaio, Í., Braga-Henriques, A., Pham, C., Ocaña, O., de Matos, V., Morato, T., Porteiro, F.M.,
1355 2012. Cold-water corals landed by bottom longline fisheries in the Azores (north-eastern
1356 Atlantic). *Journal of the Marine Biological Association of the United Kingdom* 92, 1547-
1357 1555. doi:10.1017/S0025315412000045

1358 Sanchez, F., Serrano, A., Ballesteros, M.G., 2009. Photogrammetric quantitative study of habitat and
1359 benthic communities of deep Cantabrian Sea hard grounds. *Continental Shelf Research* 29,
1360 1174-1188. 10.1016/j.csr.2009.01.004

1361 Sanchez, P., Maynou, F., Demestre, M., 2004. Modelling catch, effort and price in a juvenile *Eledone*
1362 *cirrrosa* fishery over a 10-year period. *Fisheries Research* 68, 319-
1363 327. 10.1016/j.fishres.2003.11.008

1364 Sarda, F., 1998. *Nephrops norvegicus* (L.): Comparative biology and fishery in the Mediterranean Sea.
1365 Introduction, conclusions and recommendations. *Scientia Marina* 62, 5-15

1366 Sarda, F., D'Onghia, G., Politou, C.Y., Company, J.B., Maiorano, P., Kapiris, K., 2004. Deep-sea
1367 distribution, biological and ecological aspects of *Aristeus antennatus* (Risso, 1816) in the
1368 western and central Mediterranean Sea. *Scientia Marina* 68, 117-127

1369 Sherwood, O.A., Thresher, R.E., Fallon, S.J., Davies, D.M., Trull, T.W., 2009. Multi-century time-
1370 series of ¹⁵N and ¹⁴C in bamboo corals from deep Tasmanian seamounts: evidence for stable
1371 oceanographic conditions. *Mar. Ecol. Prog. Ser.* 397, 209-218

1372 Spengler, A., Costa, M.F., 2008. Methods applied in studies of benthic marine debris. *Marine*
1373 *Pollution Bulletin* 56, 226-230. 10.1016/j.marpolbul.2007.09.040

1374 Tully, O., Hillis, J.P., 1995. Causes and spatial scales of variability in population-structure of
1375 *Nephrops norvegicus* (L.) in the Irish Sea. *Fisheries Research* 21, 329-347. 10.1016/0165-
1376 7836(94)00303-e

1377 United Nation, 2007. Resolution 61/105 adopted by the General Assembly on Sustainable fisheries,
1378 including through the 1995 Agreement for the Implementation of the Provisions of the United
1379 Nations Convention on the Law of the Sea of 10 December 1982 relating to the Conservation
1380 and Management of Straddling Fish Stocks and Highly Migratory Fish Stocks, and related
1381 instruments. Resolution 61/105 adopted by the General Assembly 61/105, ONU, 23.

1382 Wagner, D., Luck, D.G., Toonen, R.J., 2012. The biology and ecology of black corals (Cnidaria:
1383 Anthozoa: Hexacorallia: Antipatharia). *Adv Mar Biol* 63, 67-132. B978-0-12-394282-1.00002-
1384 8 [pii]
1385 10.1016/B978-0-12-394282-1.00002-8 [doi]

1386 Watremez, P., 2012. Canyon heads in the French Mediterranean Sea - Overview of results from the
1387 MEDSEACAN and CORSEACAN campaigns (2008-2010), in: Wurtz, M. (Ed.),
1388 Mediterranean Submarine Canyons: Ecology and Governance. IUCN, Gland, Switzerland, pp.
1389 105-112.

1390 Williams, B., Risk, M., Stone, R., Sinclair, D., Ghaleb, B., 2007. Oceanographic changes in the North
1391 Pacific Ocean over the past century recorded in deep-water gorgonian corals. *Marine Ecology-
1392 Progress Series* 335, 85-94. 10.3354/meps335085

1393 Zibrowius, H., 1980. Les Scléactiniaires de la Méditerranée et de l'Atlantique nord-oriental.
1394 Mémoires de l'Institut Océanographique de Monaco 11, 1-238

1395 Zibrowius, H., 2003. La communauté des "coraux blancs", les faunes des canyons et des montagnes
1396 sous-marines de la Méditerranée profonde. Plan d'Action Stratégique pour la Conservation de
1397 la Biodiversité dans la Région Méditerranéenne (PAS BIO), 43.

1398

1399
1400
1401
1402
1403
1404

Table 1

List of MEDSEACAN 2009 dives ordered by canyon. For each dive the latitude/longitude of the dive's gravity centre, the length of the navigation track, the depth (min, max, mean), the distance to the coast, the mean slope and the percentage of hard/soft substrate are mentioned. Canyons are listed from westward to eastward.

Canyon	Explored length (km)	Dive nb	Latitude	Longitude	Length (m)	Min Depth(m)	Max Depth (m)	Mean Depth (m)	Distance (degrees)	Mean slope (degree)	Hard substrate (%)	Soft substrate (%)
Lacaze-Duthiers	10.97	P2	42°33.294 N	3°24.090 E	606	240	256	248	0.2445	27	100	0
		P3	42°35.010 N	3°24.258 E	1553	200	310	255	0.2669	19	50	50
		P6	42°32.598 N	3°25.056 E	1752	200	542	371	0.2398	24	20	80
		P7	42°32.934 N	3°26.316 E	1490	183	550	367	0.2541	26	0	100
		P11	42°35.028 N	3°23.280 E	990	183	280	232	0.2535	19	50	50
		P13	42°31.152 N	3°26.388 E	2853	201	665	433	0.2292	22	0	100
		P14	42°34.794 N	3°24.336 E	595	203	360	282	0.2665	19	50	50
		P15	42°33.816 N	3°23.862 E	1131	321	385	226	0.2516	33	80	20
Pruvost	3.84	P1	42°30.618 N	3°32.646 E	1489	202	523	363	0.2924	20	0	100
		P2	42°31.980 N	3°32.928 E	1035	200	475	338	0.3100	21	0	100
		P5	42°32.454 N	3°30.444 E	316	180	235	208	0.2877	14	0	100
		P6	42°33.360 N	3°31.560 E	996	194	368	281	0.3116	17	0	100
Bourcart	6.16	P2	42°43.248 N	3°40.860 E	1359	203	463	333	0.5379	19	0	100
		P5	42°36.792 N	3°45.114 E	1584	377	625	501	0.5203	24	0	100
		P6	42°43.476 N	3°44.778 E	1669	253	403	328	0.5857	12	0	100
		BO_R2K	42°44.670 N	3°43.050 E	1549	310	360	335	0.5605	15	90	100
Marti	5.38	P1	42°43.326 N	3°57.660 E	1988	374	609	492	0.7081	24	0	100
		P2	42°47.538 N	3°55.980 E	1348	190	378	284	0.6357	15	0	100
		P4	42°47.184 N	3°57.816 E	672	226	347	287	0.6611	22	0	100
		P5	42°43.926 N	4°0.282 E	1367	329	605	467	0.7264	21	0	100
Sète	4.73	P1	42°41.976 N	4°9.606 E	1320	279	626	453	0.7610	20	0	100
		P2	42°45.696 N	4°7.932 E	1214	315	540	428	0.7026	23	0	100
		P3	42°44.718 N	4°11.298 E	1856	231	700	466	0.7151	21	0	100
		P8	42°47.892 N	4°6.534 E	338	180	235	208	0.6701	4	0	100
Montpellier	8.96	P1	42°48.906 N	4°22.548 E	3495	200	700	450	0.5817	20	0	100
		P2	42°47.640 N	4°24.504 E	1550	185	613	399	0.5901	26	0	100
		P3	42°45.456 N	4°23.472 E	2038	260	600	430	0.6293	22	0	100
		P4	42°49.134 N	4°26.874 E	1881	200	402	301	0.5555	10	0	100
Petit-Rhône	9.24	P1	42°58.038 N	4°29.010 E	1899	343	408	376	0.4033	4	0	100
		P3	42°55.212 N	4°30.780 E	2367	180	487	334	0.4413	27	0	100
		P4	42°51.882 N	4°39.930 E	1891	268	600	434	0.4800	16	0	100
		P5	42°50.316 N	4°29.340 E	3084	206	627	417	0.5265	14	0	100
Grand-Rhône	5.83	P1	42°54.738 N	4°45.336 E	1794	180	420	300	0.4232	13	0	100
		P2	42°55.116 N	4°50.232 E	1669	190	427	309	0.4100	17	0	100
		P3	42°58.134 N	4°47.778 E	2366	410	443	427	0.3620	15	0	100
Couronne	10.40	P1	43°2.250 N	5°1.518 E	1804	202	571	387	0.2870	17	0	100
		P2	43°3.330 N	5°6.918 E	1896	200	500	350	0.2600	14	0	100
		P3	43°3.960 N	5°8.256 E	1299	203	501	352	0.2365	18	0	100
		P4	43°0.354 N	5°1.242 E	1962	209	551	380	0.3194	18	0	100
		P5	43°1.890 N	5°4.302 E	2118	275	550	413	0.2924	13	0	100
		P6	43°0.618 N	5°7.848 E	1324	325	542	434	0.2800	18	0	100
Planier	17.90	P1	43°6.108 N	5°12.372 E	1033	213	420	317	0.1613	20	60	40

		P2	43°5.316 N	5°12.540 E	728	338	554	446	0.1683	32	90	10
		P3	43°4.386 N	5°13.194 E	983	309	640	475	0.1737	29	50	50
		P4	43°3.882 N	5°8.400 E	2553	180	585	383	0.2361	19	0	100
		P5	43°5.982 N	5°13.938 E	528	418	486	452	0.1445	11	0	100
		P6	43°7.188 N	5°12.684 E	1517	180	313	247	0.1449	13	10	90
		P7	43°6.432 N	5°12.456 E	3954	200	452	326	0.1571	18	70	20
		P8	43°6.552 N	5°14.526 E	675	340	390	365	0.1319	11	60	40
		P9	43°4.944 N	5°11.670 E	1884	200	593	397	0.1838	21	10	90
		P10	43°5.376 N	5°14.082 E	1868	232	425	329	0.1509	12	0	100
		P11	43°6.732 N	5°14.514 E	859	195	340	268	0.1289	14	50	50
		P12	43°5.718 N	5°12.642 E	498	225	439	332	0.1641	34	90	10
		P13	43°5.496 N	5°12.564 E	824	266	413	340	0.1655	34	90	10
Cassidaigne	8.12	P1	43°6.756 N	5°27.630 E	2179	205	215	210	0.0863	19	100	0
		P2	43°2.598 N	5°24.048 E	1327	448	634	541	0.1282	41	100	0
		P3	43°2.808 N	5°23.850 E	1210	285	470	378	0.1241	27	80	20
		P4	43°5.364 N	5°25.752 E	767	180	386	283	0.0899	29	70	30
		P6	43°8.028 N	5°28.158 E	855	210	465	338	0.0672	22	20	80
		P7	43°1.272 N	5°29.184 E	900	200	470	335	0.1729	36	60	40
		P8	43°3.636 N	5°29.400 E	879	214	508	361	0.1361	33	60	40
La Ciotat	7.25	P1	43°1.404 N	5°43.254 E	2091	180	600	390	0.0738	30	80	20
		P2	43°0.498 N	5°40.848 E	1350	180	498	339	0.1122	20	80	20
		P3	42°58.746 N	5°42.024 E	2492	216	583	400	0.1206	19	20	80
		P5	42°57.780 N	5°38.028 E	1318	180	518	349	0.1771	24	40	60
Sicié	8.70	P1	43°0.846 N	5°52.542 E	1449	180	398	289	0.0358	22	40	60
		P2	42°59.538 N	5°54.630 E	1446	180	486	333	0.0736	32	30	70
		P4	43°0.972 N	5°53.604 E	1516	180	580	380	0.0453	32	40	60
		P5	42°59.958 N	5°51.612 E	2460	180	560	370	0.0480	27	10	90
		P7	43°0.936 N	5°52.434 E	529	180	280	230	0.0331	20	50	50
		P8	43°0.660 N	5°55.038 E	1296	185	420	303	0.0560	31	70	30
Toulon	7.75	P4	43°24.048 N	6°55.212 E	2021	180	731	456	0.0382	24	30	70
		P5	43°2.346 N	5°58.158 E	1502	180	547	364	0.0369	20	40	60
		P6	42°58.416 N	5°57.000 E	2033	190	687	439	0.0921	22	90	10
		P7	43°1.932 N	6°0.198 E	2192	180	593	387	0.0487	25	40	60
Open slope	17.69	PO_P1	42°56.838 N	6°16.866 E	651	402	645	524	0.0611	30	90	10
		PO_P5	42°57.624 N	6°19.938 E	1332	180	627	404	0.0533	40	40	60
		PO_P6	42°56.400 N	6°14.076 E	2285	202	418	310	0.0494	27	30	70
		PO_P8	42°56.646 N	6°6.426 E	3230	195	710	453	0.0764	28	20	80
		PO_P9	42°56.862 N	6°14.982 E	2244	200	705	453	0.0481	29	60	40
		PO_P10	42°56.280 N	6°7.914 E	1748	317	557	437	0.0671	17	30	70
		MG_P10	43°1.488 N	6°38.742 E	1332	250	598	424	0.1358	32	20	80
		MG_P11	42°57.840 N	6°21.234 E	1516	180	800	490	0.0367	36	60	40
		MG_P16	43°0.060 N	6°32.088 E	1804	224	548	386	0.0501	32	70	30
		MG_P17	43°0.210 N	6°29.766 E	1544	180	673	427	0.0268	35	70	30
Stoechades	7.39	MG_P3	43°4.362 N	6°31.674 E	1515	252	707	480	0.0283	32	40	60
		MG_P4	43°3.846 N	6°28.266 E	695	180	394	287	0.0161	20	0	100
		MG_P5	43°8.730 N	6°40.686 E	1283	180	722	451	0.0361	30	40	60
		MG_P6	43°8.058 N	6°33.738 E	1200	200	515	358	0.0397	21	0	100
		MG_P7	43°5.244 N	6°26.916 E	558	300	322	311	0.0465	6	0	100
		MG_P14	43°4.470 N	6°34.296 E	956	302	652	477	0.0662	34	10	90
		MG_P15	43°8.868 N	6°37.368 E	1180	200	524	362	0.0100	32	70	30

Cannes	11.15	P3	43°29.754 N	7°1.236 E	2905	180	692	436	0.0189	29	10	30
		P4	43°29.784 N	6°58.824 E	2440	180	537	359	0.0240	32	50	50
		P5	43°30.744 N	6°58.716 E	1680	200	484	342	0.0242	23	0	100
		P6	43°28.794 N	7°3.516 E	4128	180	631	406	0.0260	32	0	100
Var	15.47	P1	43°40.656 N	7°17.238 E	6332	180	700	440	0.0100	26	20	80
		P2	43°39.930 N	7°20.790 E	2279	180	355	268	0.0144	17	10	90
		P6	43°40.932 N	7°17.610 E	324	180	290	235	0.0028	38	100	0
		P10	43°35.748 N	7°10.434 E	2455	315	586	451	0.0428	24	40	60
		P11	43°35.898 N	7°9.918 E	4082	180	456	318	0.0354	29	20	80

1405
1406
1407
1408
1409
1410
1411
1412
1413
1414
1415
1416

Table 2

List of additional dives processed for qualitative information in the Lacaze-Duthiers and Cassidaigne canyons. For each dive the length of the navigation track, the latitude of the dive's gravity centre, the longitude of the dive's gravity centre and the depth (min, max, mean) are mentioned.

Canyon	Cruise	Dive nb	Latitude	Longitude	Length (m)	Min Depth(m)	Max Depth (m)	Mean Depth (m)
Lacaze-Duthiers	Marum Senckenberg 2011 Super Achille ROV	D1	42°33.553 N	3°25.540 E	847	250	450	350
		D2	42°33.677 N	3°23.945 E	35	300	350	325
		D3	42°33.675 N	3°23.953 E	1905	325	325	325
		D5	42°28.300 N	3°27.300 E	1905	200	600	400
		D6	42°33.100 N	3°24.460 E	494	250	450	350
		D7	42°33.110 N	3°24.451 E	249	250	400	375
		Cassidaigne	Marum 2009 Super Achille ROV	D1	43°7.094 N	5°28.404 E	97	460
D2	43°6.507 N			5°27.249 E	2745	184	240	212
D3	43°3.170 N			5°28.602 E	963	516	564	540
D4	43°3.280 N			5°29.905 E	1670	231	419	325
D5	43°6.603 N			5°26.756 E	1561	198	370	284
D6	43°6.810 N			5°25.930 E	1070	134	280	207
D7	43°6.712 N			5°27.153 E	2101	243	465	354
D8	43°6.583 N			5°27.227 E	307	187	237	212
D9	43° 4.102 N			5°25.519 E	1289	246	454	350
Marum 2009 Remora submersible	R1		43° 6.977 N	5° 28.120 E	3851	320	530	425
	R2		43° 3.103 N	5° 24.978 E	5557	250	500	375
	R3		43° 7.060 N	5° 30.321 E	3774	230	530	380
	R4		43° 6.834 N	5° 27.925 E	2323	280	400	340
Ifremer Cyatox 1995 Cyana Submersible	1214-03		43°7.000 N	5° 27.000 E	6276	292	646	469
Ifremer ESSROV 2010 Victor 6000 ROV	397-01		43° 7.009 N	5° 28.162 E	998	251	400	326
	401-05		43° 6.473 N	5° 27.284 E	4248	60	284	172
	407-11		43° 7.206 N	5° 28.846 E	3216	601	750	676

1417
1418
1419
1420
1421

1422
1423
1424
1425
1426
1427

Table 3

List of fishes observed during MEDSEACAN 2009 cruise classified in three categories: Marketable (M), Edible (E) and Others (O). The total abundance and maximum depth at which they were observed is mentioned. (M*) *Trachurus* sp. is a pelagic marketable species that has been removed from the following of the study.

Class Order	Family	Genus species	Total effectif observed	Maximum Depth (m)	M	E	O	English name	French name
Actinopterygii									
Anguilliformes		sp. gen.	1	442			O		
	Congridae	<i>Conger conger</i>	23	555		E		Conger	Congre
Aulopiformes	Chlorophthalmidae	<i>Chlorophthalmus agassizi</i>	8	464			O		
	Synodontidae	<i>Synodus saurus</i>	1	330			O		
Beryciformes	Trachichthyidae	<i>Hoplostethus mediterraneus</i>	29	599			O		
Gadiformes	Gadidae	<i>Gadiculus argenteus</i>	127	504			O		
		<i>Lepidion lepidion</i>	1	686		E		Mediterranean codling	Morue Méditerranéenne
		<i>Micromesistius poutassou</i>	16	655	M			Poutassou / blue whiting	Merlan bleu
	Lotidae	<i>Molva macrophthalma</i>	6	448		E		Spanish ling	Lingue espagnole
	Macrouridae	sp. gen.	28	709			O		
		<i>Coelorinchus caelorhincus</i>	192	579			O		
		<i>Hymenocephalus italicus</i>	15	617			O		
		<i>Nezumia aequalis</i>	16	708			O		
		<i>Trachyrincus scabrus</i>	23	696			O		
	Merlucciidae	<i>Merluccius merluccius</i>	57	645	M			Hake	Merlu / Colin
	Moridae	sp. gen.	5	618			O		
	Phycidae	<i>Phycis blennoides</i>	140	689		E		Greater forkbeard	Mostelle blanche de vase
		<i>Phycis phycis</i>	2	360		E		Forkbeard	Mostelle brune de roche
		<i>Phycis</i> sp.	4	320		E		Forkbeard	Mostelles
Lophiiformes	Lophiidae	<i>Lophius piscatorius</i>	8	456	M			Monkfish	Lotte / Baudroie
Myctophiformes	Myctophidae	sp. gen.	21	670			O		
Notacanthiformes	Notacanthidae	<i>Notacanthus bonaparte</i>	7	619			O		
Ophidiiformes		sp. gen.	4	473			O		
	Carapidae	<i>Echiodon dentatus</i>	1	431			O		
	Ophidiidae	<i>Benthocometes robustus</i>	5	634			O		
Osmeriformes	Argentinidae	<i>Argentina sphyraena</i>	57	408			O		
Perciformes	Callionymidae	<i>Synchiropus phaeton</i>	2	347			O		
	Caproidae	<i>Capros aper</i>	126	431			O		
	Carangidae	<i>Trachurus</i> sp.	shoals	488	M*			Horse mackerel	Chinchard
	Epigonidae	<i>Epigonus denticulatus</i>	5	491			O		
		<i>Epigonus telescopus</i>	2	423			O		
	Labridae	<i>Acantholabrus palloni</i>	35	381			O		
	Mullidae	<i>Mullus barbatus</i>	1	208		E		Red mullet	Rouget barbet (de vase)
		<i>Mullus</i> sp.	3	320		E			
	Polyprionidae	<i>Polyprion americanus</i>	3	627	M			Wreckfish	Cemier
	Serranidae	<i>Anthias anthias</i>	shoals	239			O		
	Sparidae	sp. gen.	1	250			O		
		<i>Pagellus</i> sp.	13	403	M			Sea-bream	Pageot
	Trichiuridae	sp. gen.	45	545	M			Cutlassfishes	Sabres
Pleuronectiformes	Scophthalmidae	<i>Lepidorhombus boscii</i>	56	580		E		Four spotted megrim	Cardine à 4 tâches
		<i>Lepidorhombus whiffiagonis</i>	5	302		E		Megrim	Cardine franche
Scorpaeniformes	Peristediidae	<i>Peristedion cataphractum</i>	4	342			O		
	Scorpaenidae	<i>Scorpaena scrofa</i>	50	465	M			Red scorpionfish	Rascasse rouge
	Sebastidae	<i>Helicolenus dactylopterus</i>	482	614		E		Blackbelly rosefish	Sebaste chèvre
	Triglidae	sp. gen.	22	476	M			Gurnards	Grondins

		<i>Trigla lyra</i>	77	488	M	Piper gumard	Grondin lyre
Stomiiformes	Stomiidae	sp. gen.	1	705		O	
		<i>Chauliodus sloani</i>	3	593		O	
		<i>Stomias boa</i>	2	578		O	
Syngnathiformes	Centriscidae	<i>Macroramphosus scolopax</i>	3	262		O	
Zeiformes	Zeidae	<i>Zeus faber</i>	1	243	M		
Elasmobranchii			11	690		O	
Carcharhiniformes	Scyliorhinidae	<i>Scyliorhinus canicula</i>	35	394	M	Lesser spotted dogfish	Petite roussette / saumonette
		<i>Scyliorhinus</i> sp.	3	379	M		Roussettes
	Triakidae	<i>Galeus melastomus</i>	91	505		E	Black-mouthed dogfish Chien espagnol
Hexanchiformes	Hexanchidae	<i>Hexanchus griseus</i>	1	366		O	
Rajiformes	Rajidae	<i>Raja</i> sp.	1	478		O	
Squaliformes	Dalatiidae	sp. gen.	4	481		O	
		<i>Etmopterus spinax</i>	27	587		O	
		<i>Oxynotus centrina</i>	1	225		O	
Holocephali							
Chimaeriformes	Chimaeridae	<i>Chimaera monstrosa</i>	28	584		O	

1428